SEMMELWEIS EGYETEM
DOKTORI ISKOLA

Ph.D. értekezések

3468.

HORVÁTH MÁRTON

Szív- és érrendszeri betegségek élettana és klinikuma
című program

Programvezető: Dr. Merkely Béla, egyetemi tanár
Témavezető: Dr. Szűcs Andrea, egyetemi docens

Left Ventricular Excessive Trabeculation: Insights from Multimodality Imaging and Novel Approaches to Right Ventricular Assessment

PhD thesis

Márton Horváth MD

Theoretical and Translational Medicine Doctoral School
Semmelweis University

Supervisor:	Andrea Szűcs MD, Ph.D
Official reviewers:	Astrid Apor, MD, Ph.D
	Csaba Jenei, MD, Ph.D

Head of the Complex Examination Committee:	György Reusz, MD, DSc.
Members of the Complex Examination Committee:	Zoltán Prohászka MD, DSc.
	Mihály Kovács MD, DSc.

Budapest
2026

Table of Contents

List of Abbreviations

2D TTE: two-dimensional transthoracic echocardiography

2D-STE: two-dimensional speckle-tracking echocardiography

3DE: three-dimensional echocardiography

3D-STE: three-dimensional speckle-tracking echocardiography

AEF: anteroposterior ejection fraction

AF: atrial fibrillation

AV: atrioventricular

bSSFP: balanced steady-state free precession

CMR: Cardiac Magnetic Resonance

ECM: extracellular matrix

EDV: end-diastolic volume

EF: ejection fraction

ESV: end-systolic volume

FWLS: free-wall longitudinal strain

FT-CMR: feature-tracking cardiac magnetic resonance imaging

GAS: global area strain

GCS: global circumferential strain

GLS: global longitudinal strain

HF: heart failure

ICC: intraclass correlation coefficient

ICD: implantable cardioverter defibrillator

IV: intraventricular

LGE: late gadolinium enhancement

LEF: longitudinal ejection fraction

LV: left ventricle

LVET: left ventricular excessive trabeculation

LVNC: left ventricular noncompaction

MESA: Multi-Ethnic Study of Atherosclerosis

NCC: non-compacted to compacted myocardial thickness ratio

OAC: oral anticoagulant

PE: percentage error

PM: pacemaker

QMass: Medis software modul

QStrain: Medis software modul

REF: radial ejection fraction

RV: right ventricle

SAX: short-axis

SLS: septal longitudinal strain

SPSS: IBM statistical software

SV: stroke volume

TE: thromboembolism

TIA: transient ischemic attack

TTE: transthoracic echocardiography

VA: ventricular arrhythmias

VES: ventricular extrasystole

1. Introduction

1.1 Normal myocardial structure

The human myocardium is a complex, highly organized tissue that serves both mechanical and electrophysiological functions essential for maintaining cardiac output and systemic perfusion. It is composed primarily of cardiac myocytes, specialized interstitial cells, an extracellular matrix (ECM), and an extensive network of capillaries, all of which are arranged in a precise three-dimensional architecture [1].

At the microscopic level, cardiac myocytes are elongated, striated cells containing highly organized sarcomeres composed of actin and myosin filaments, which interact through cross-bridge cycling regulated by calcium-dependent troponin-tropomyosin mechanisms [2]. The myocytes are interconnected through intercalated discs containing desmosomes, adherens junctions, and gap junctions, which facilitate mechanical coupling and electrical impulse propagation across the myocardium [3].

The ECM plays a structural and regulatory role, providing tensile strength through fibrillar collagen and influencing myocyte alignment, as well as modulating mechano-electric coupling [4]. The capillary network within the myocardium ensures a high capillary-to-myocyte ratio, supporting the elevated oxidative metabolic demands of the myocardium [5].

From a macroscopic perspective, the ventricular wall is composed of three principal layers: the endocardial, myocardial, and epicardial layers, which together facilitate systolic ejection and diastolic filling [6]. Fiber orientation gradually transitions from a right-handed helix in the subendocardium, through approximately circumferentially oriented fibers in the midwall, to a left-handed helix in the subepicardium. The transmural helical orientation of the myocardial fibers maintains coordinated torsional (twisting and untwisting) movements that maximize the efficiency of LV ejection and, importantly, also filling due to their consequential suction effect [7, 8] [**Figure 1**].

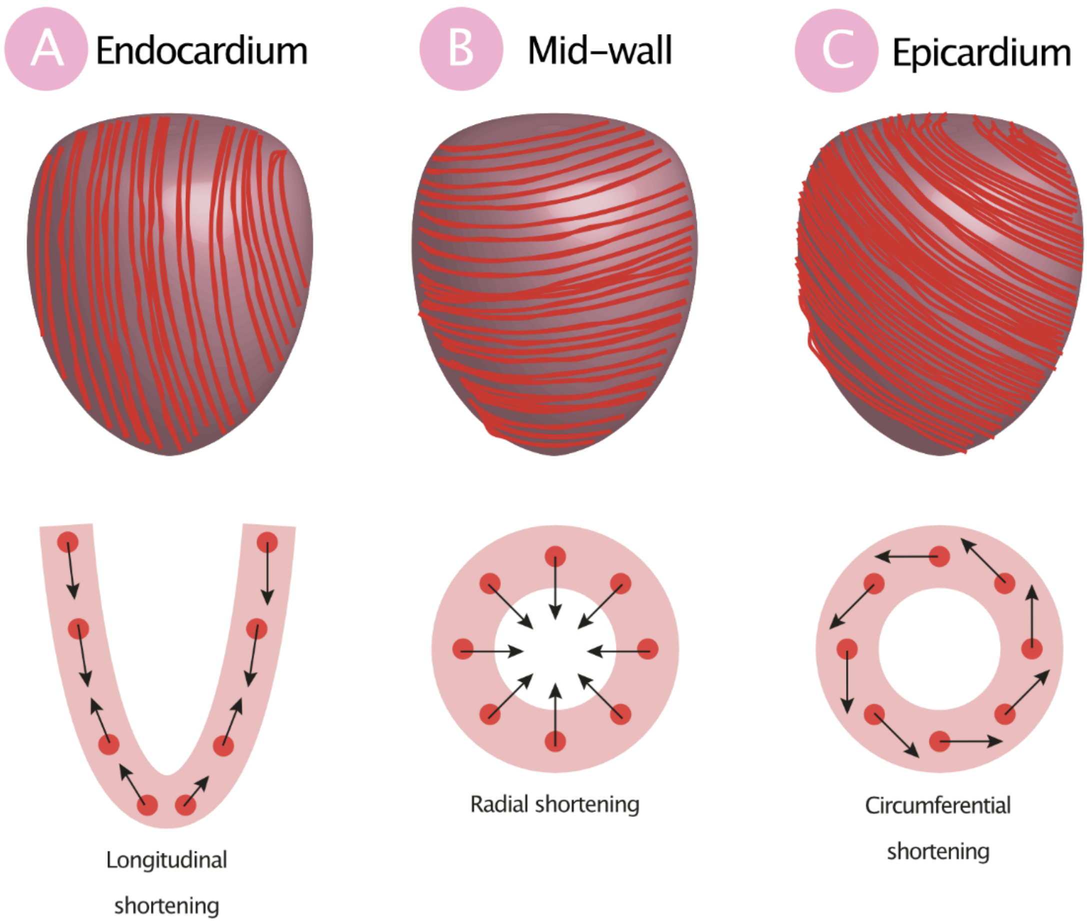

Figure 1. Myocardial fiber orientation and principal components of ventricular shortening.

A: Subendocardial fibers are oriented in a right-handed helical pattern, which generates longitudinal shortening during systole. B: Mid-wall fibers are arranged circumferentially, contributing to radial thickening. C: Subepicardial fibers follow a left-handed helical pattern, resulting in circumferential shortening and ventricular twisting.

Source: https://ecgwaves.com/topic/structure-and-function-of-myocardial-fibers-myocardium/

During embryonic development, the myocardium forms a trabeculated, sponge-like network that is capable of adequate oxygen diffusion before the formation of the coronary circulation. Between weeks 5 and 12 of gestation, the compact and trabeculated myocardial layers undergo partially independent growth trajectories, consistent with the allometric growth paradigm. This challenges the earlier theory that the trabecular layer originates directly from compact layer condensation. Instead, converging evidence from morphometric analyses in both animal and human models, together with mechanistic investigations, has reshaped our understanding of this developmental process [**Figure 2**].

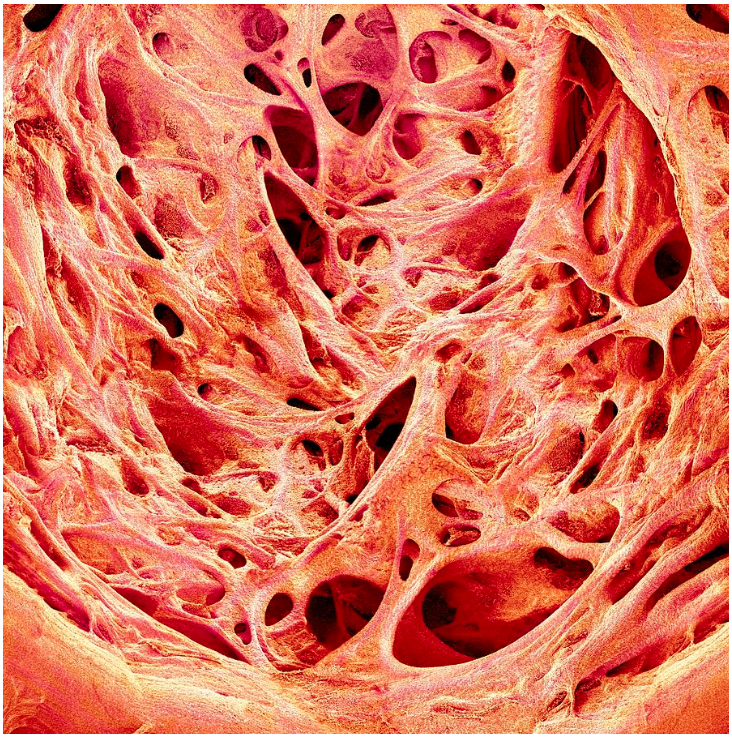

***Figure 2*. Scanning electron micrograph of the ventricular endocardial surface during early cardiac morphogenesis, highlighting the physiological trabecular meshwork.**

Source: https://www.sciencephoto.com/

Despite the predominance of compact myocardium in adults, trabeculated structures persist physiologically in the apical and lateral segments of the left ventricle (LV), as well as in the right ventricle. Myocardial trabeculation refers to the muscular ridges that protrude from the endocardial surface into the ventricular cavity, forming a reticulated inner architecture. In the normally developed heart, this trabecular meshwork becomes less prominent and integrates with the compact myocardium, while still contributing to ventricular mechanics, namely by optimizing filling dynamics and wall stress distribution.

The right ventricle is physiologically more trabeculated than the left one, with prominent trabeculations in the apical and inferior walls, as well as around the moderator band and septomarginal trabeculation, reflecting its adaptation to accommodate preload variations at low pulmonary pressures [9-11].

The functional integration of compact and trabeculated myocardium is essential for normal ventricular mechanics and electrophysiology. Disruption of this balance, whether through excessive or hypotrabeculation, impaired myocardial compaction, or abnormal fiber orientation, can lead to altered strain patterns, reduced contractile reserve, and a heightened susceptibility to arrhythmia [12, 13].

1.2 Understanding the definition of hypertrabeculation

The concept of hypertrabeculation refers to the extent of trabecular prominence that exceeds what is typically observed in a given ventricle. When present in the LV, it is increasingly referred to as left ventricular excessive trabeculation (LVET), in line with the terminology of the novel 2023 ESC cardiomyopathy guidelines [13].

It is worth noting that this guideline and the 2023 JACC Imaging Expert Panel explicitly emphasize that excessive trabeculation should be considered a morphological phenotype rather than a distinct cardiomyopathy, thereby aligning clinical interpretation with developmental biology evidence [12-14].

Population-based imaging studies also demonstrate that this morphological trait is not confined to patients with cardiomyopathy. The MESA (Multi-Ethnic Study of

Atherosclerosis) cohort, which included asymptomatic adults free of clinical cardiovascular disease and hypertension, showed that up to 43% of individuals fulfilled the Petersen CMR criterion (non-compacted to compacted ratio > 2.3) in at least one myocardial segment [15]. Depending on the applied diagnostic thresholds and methodology, the prevalence of excessive trabeculation in the general population has been estimated between 20% and 43% [12, 16-18] [**Figure 3**]. These findings emphasize that LVET should be considered a morphological phenotype that may represent a physiological variant or, in certain contexts, a marker of pathological remodeling rather than a distinct cardiomyopathy [13].

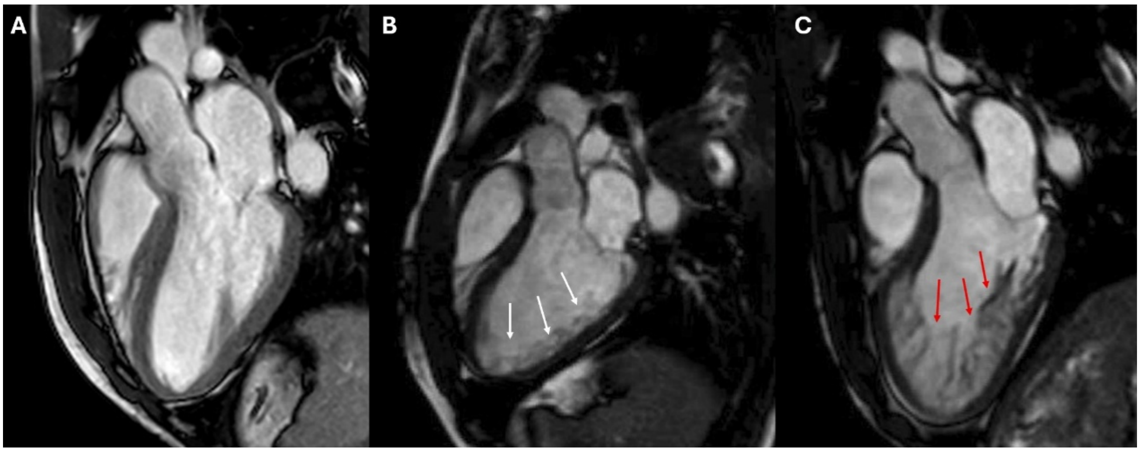

Figure 3. Spectrum of left ventricular trabeculation on cardiac magnetic resonance imaging.

A: Heart with normal amount of trabeculation.

B: Heart with increased trabeculation (white arrows) not fulfilling diagnostic criteria.

C: Definitive excessive trabeculation (red arrows), showing a bilayered myocardial structure with a thin compacted epicardial and a prominent non-compacted endocardial layer with deep intertrabecular recesses, consistent with established diagnostic criteria.

Source: Semmelweis University

However, excessive trabeculation may manifest as a pathological phenotype, commonly referred to as LV hypertrabeculation/non-compaction, observed in congenital, genetic, or acquired conditions [13, 19, 20].

1.2.1. Hypertrabeculation of the left ventricle

From a genetic perspective, left ventricular excessive trabeculation (LVET) has been associated with variants in sarcomeric protein genes such as *MYH7*, *MYBPC3*, and *TTN*, as well as in cytoskeletal and mitochondrial genes [21]. The phenotype is highly heterogeneous, with incomplete penetrance and variable expression even within families, supporting the concept that LVET represents a morphological trait rather than a single disease entity. Beyond primary genetic causes, LVET may also present as a secondary or acquired phenomenon. Physiological hypertrabeculation has been documented under increased preload and cardiac remodeling conditions. In pregnancy, for example, approximately 25% of healthy women develop de novo LV trabeculations during gestation, and around 8% fulfill LV non-compaction criteria, most of which resolve postpartum [22]. In competitive athletes, the prevalence of trabecular criteria by echocardiography ranges between 1.4% and 8.1%, depending on definition and ethnicity [17]. These observations suggest that increased trabeculation may arise as an adaptive remodeling response in highly trained individuals [23].

Pathological secondary LVET has been associated with various systemic and cardiac conditions. Hematological disorders such as β-thalassemia and sickle-cell disease, chronic kidney disease, and endocrine disturbances (e.g., hyperthyroidism) have been associated with LVET, possibly reflecting an adaptive response to altered hemodynamic loads or metabolic stress [17, 23]. Certain neuromuscular disorders and congenital cardiac anomalies (e.g., Barth syndrome, Ebstein anomaly, tetralogy of Fallot) also frequently demonstrate trabecular prominence, suggesting remodeling rather than primary development defects [13].

Overall, recognizing LVET as a heterogeneous morphological phenotype with diverse genetic, physiological, and pathological underpinnings is essential for clinical interpretation. This framework aligns imaging findings with developmental and adaptation biology. It ensures that risk stratification and management decisions rely not only on trabecular morphology, but on a comprehensive integration of clinical context, family history, genetics, and functional assessment.

1.2.2. Hypertrabeculation of the right ventricle

The right ventricle (RV) is physiologically more trabeculated than the LV, even in healthy individuals. Prominent trabeculations are particularly evident in the apical and inferior walls, as well as in the region of the moderator band and septomarginal trabeculation [24]. This structural characteristic is thought to optimize the role of the RV in accommodating large variations in preload while maintaining low-pressure pulmonary circulation [25] [**Figure 4**].

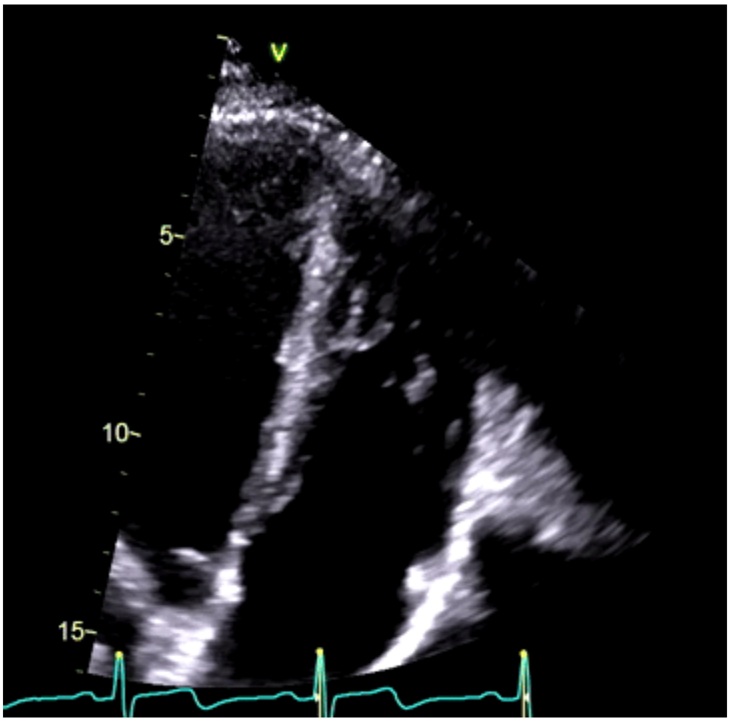

Figure 4. Two-dimensional transthoracic echocardiographic image of the right ventricle.

The apical four-chamber view demonstrates a markedly trabeculated right ventricle, consistent with hypertrabeculated morphology, underscoring the structural complexity of this chamber.

Source: Semmelweis University Heart and Vascular Center

Because of this baseline trabeculation, morphological criteria alone are not sufficient to identify pathological excessive trabeculation in the RV. Unlike in the LV, where specific ratio-based thresholds can be applied, the natural variability of RV trabeculation and the absence of universally accepted diagnostic cut-offs make purely anatomical assessment challenging [12]. However, research by Kiss et al. suggests that patients with certain LVET phenotypes may also have right ventricular non-compaction, which may be associated with subclinical RV dysfunction without causing more severe clinical symptoms [26]. Differentiating physiological trabecular prominence from pathological remodeling requires the integration of advanced imaging parameters, including volumetric analysis, myocardial strain assessment, and motion pattern evaluation.

1.3. Hypertrabeculation in the context of the updated cardiomyopathy guidelines

The 2023 European Society of Cardiology (ESC) Guidelines on cardiomyopathies represent a substantial conceptual shift in the clinical approach to LVET . Recent recommendations no longer recognize left ventricular non-compaction as a distinct cardiomyopathy, overturning earlier classifications that considered it a separate disease entity. Instead, they define LVET as a morphological feature present across a spectrum of clinical contexts, spanning physiological to pathological states [13]. This change reflects growing evidence that hypertrabeculation alone, in the absence of other structural or functional abnormalities, is not sufficient to establish a cardiomyopathy diagnosis. Large population studies, such as the previously mentioned MESA cohort, further support this view by demonstrating that between 20% and 43% of asymptomatic adults fulfill CMR criteria for excessive trabeculation, underscoring the need to interpret imaging findings in a clinical context [15].

A critical implication of this redefinition is its impact on risk stratification. The guideline emphasizes that the prognostic significance of LVET depends on the presence and severity of additional clinical and imaging markers [**Table 1, Figure 5**].

Table 1. Key domains of risk stratification in left ventricular excessive trabeculation.

Risk domain	Key markers
Ventricular function	Reduced ejection fraction, regional wall motion abnormalities, abnormal deformation indices
Tissue characterization	Presence of non-ischemic late gadolinium enhancement (LGE) or other CMR markers of fibrosis, associated with adverse remodeling and arrhythmic risk
Arrhythmic burden	Ventricular tachyarrhythmias, high-grade conduction disease, frequent premature ventricular contractions
Thromboembolic risk	Prior embolic events, imaging evidence of mural thrombus
Family history	Sudden cardiac death, cardiomyopathy, or unexplained heart failure in first-degree relatives
Genetic profile	Pathogenic variants in cardiomyopathy-associated genes, informing prognosis and guiding family screening

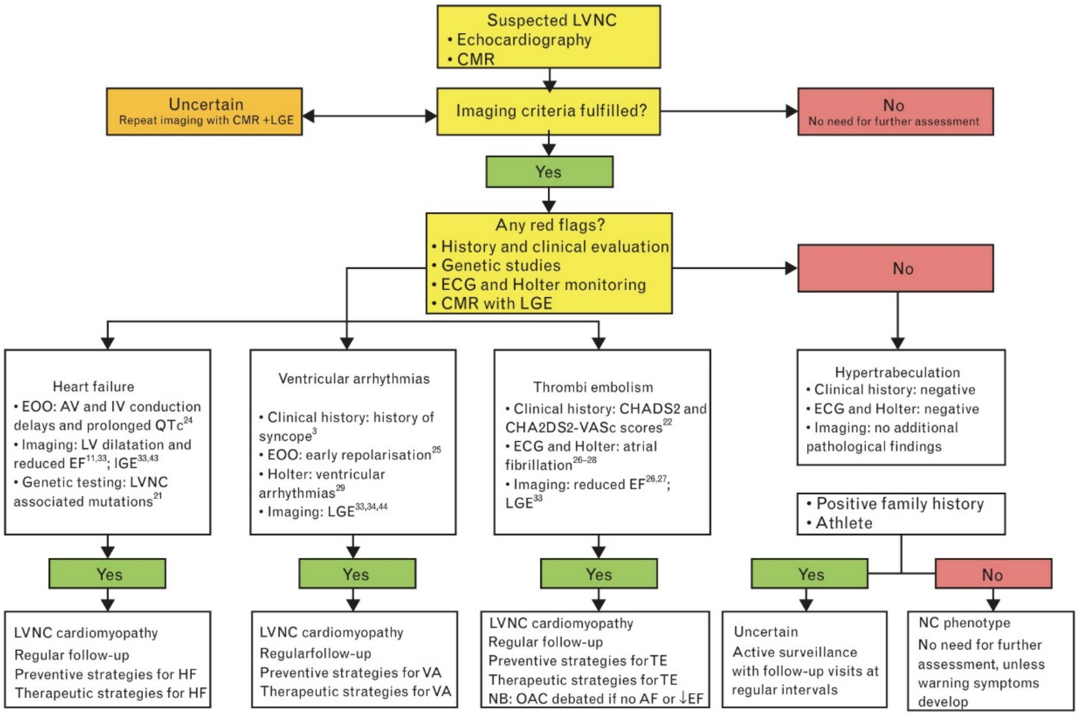

Figure 5. Risk stratification algorithm proposed by Vergani et al. for patients with suspected LVET.

The flowchart integrates imaging criteria, clinical history, arrhythmic burden, genetic testing, and tissue characterization with late gadolinium enhancement (LGE) to differentiate benign hypertrabeculation from the LVET morpholohy or the noncompaction cardiomyopathy, requiring closer follow-up and therapeutic interventions.

Abbreviations: AF: atrial fibrillation; AV: atrioventricular; CHA_2DS_2-VASc: Congestive heart failure, Hypertension, Age ≥75 years, Diabetes mellitus, Stroke or transient ischemic attack, Vascular disease, Age 65–74 years, Sex category score; CMR: cardiac magnetic resonance imaging; ECG: electrocardiography; EF: ejection fraction; HF: heart failure; IV: intraventricular; LGE: late gadolinium enhancement; LV: left ventricle; LVNC: left ventricular noncompaction; NC: noncompaction; OAC: oral anticoagulant; QTc: corrected QT interval; TE: thromboembolism; VA: ventricular arrhythmias.

Source: [27]

This multiparametric approach allows clinicians to distinguish low-risk individuals, in whom LVET is likely a benign morphological variant (e.g., in athletes or during pregnancy), from those at elevated risk, where LVET is a marker of an underlying cardiomyopathic process with prognostic relevance. Importantly, the guideline advocates for periodic reevaluation, as phenotype and risk profile may evolve over time.

Another notable change is the explicit recommendation to avoid overreliance on trabecular quantification alone, given the limited specificity of existing echocardiographic and CMR criteria. Instead, imaging findings should be interpreted in the context of the complete clinical picture. Echocardiography remains the first-line modality for assessing chamber size, function, and hemodynamics, while cardiovascular magnetic resonance (CMR) is recommended when echocardiographic data are inconclusive or when tissue characterization and scar detection may alter management. This is particularly relevant in LVET, where LGE patterns may reclassify patients into other cardiomyopathy subtypes, such as non-dilated LV cardiomyopathy, thereby influencing both risk stratification and therapeutic decision-making.

By reframing LVET as a morphological sign rather than a standalone diagnosis, the 2023 ESC Guidelines provide a framework in which hypertrabeculation is a starting point for systematic evaluation, not an end in itself. This paradigm underscores the central role of integrated clinical, genetic, and imaging-based risk assessment, and naturally leads to the following discussion on modalities for visualizing myocardial hypertrabeculation, where the technical aspects and diagnostic performance of different imaging techniques will be examined in detail. Beyond morphology, functional analysis has emerged as a critical component of the diagnostic and prognostic work-up, providing insights into ventricular mechanics, myocardial deformation, and contractile reserve that cannot be inferred from trabecular patterns alone. Modern echocardiographic techniques such as three-dimensional volumetry and speckle-tracking strain analysis, as well as advanced CMR tools including feature-tracking strain and tissue mapping, enable quantification of subtle ventricular dysfunction even when global ejection fraction is preserved [28, 29].

1.4. Modalities for visualizing myocardial hypertrabeculation

The diagnosis of LVET is mostly based on cardiac imaging modalities, most commonly echocardiography and CMR. Although the novel ESC guidelines reframed LVET as a morphological phenotype, the established imaging thresholds proposed by Jenni, Petersen, and Jacquier remain unchanged and continue to serve as reference standards in clinical and research practice [16, 20, 30]. These criteria provide objective cutoffs but have limited specificity, as excessive trabeculation can also be observed in healthy individuals. Consequently, imaging findings should always be interpreted in conjunction with functional assessment, clinical presentation, and family history [13].

1.4.1. Magnetic resonance imaging

Cardiac magnetic resonance (CMR) is regarded as the reference standard for morphological assessment of myocardial trabeculation due to its high spatial resolution, tomographic coverage, and tissue characterization [**Figure 6**].

Several quantitative criteria have been proposed:

- Petersen criterion: non-compacted to compacted (NC/C) myocardium thickness ratio >2.3 in diastole [16].
- Jacquier criterion: trabeculated LV mass >20% of total LV mass [30].
- Grothoff modification: segmental NC/C ratios with a cut-off >2.3 in multiple segments to improve specificity [31].

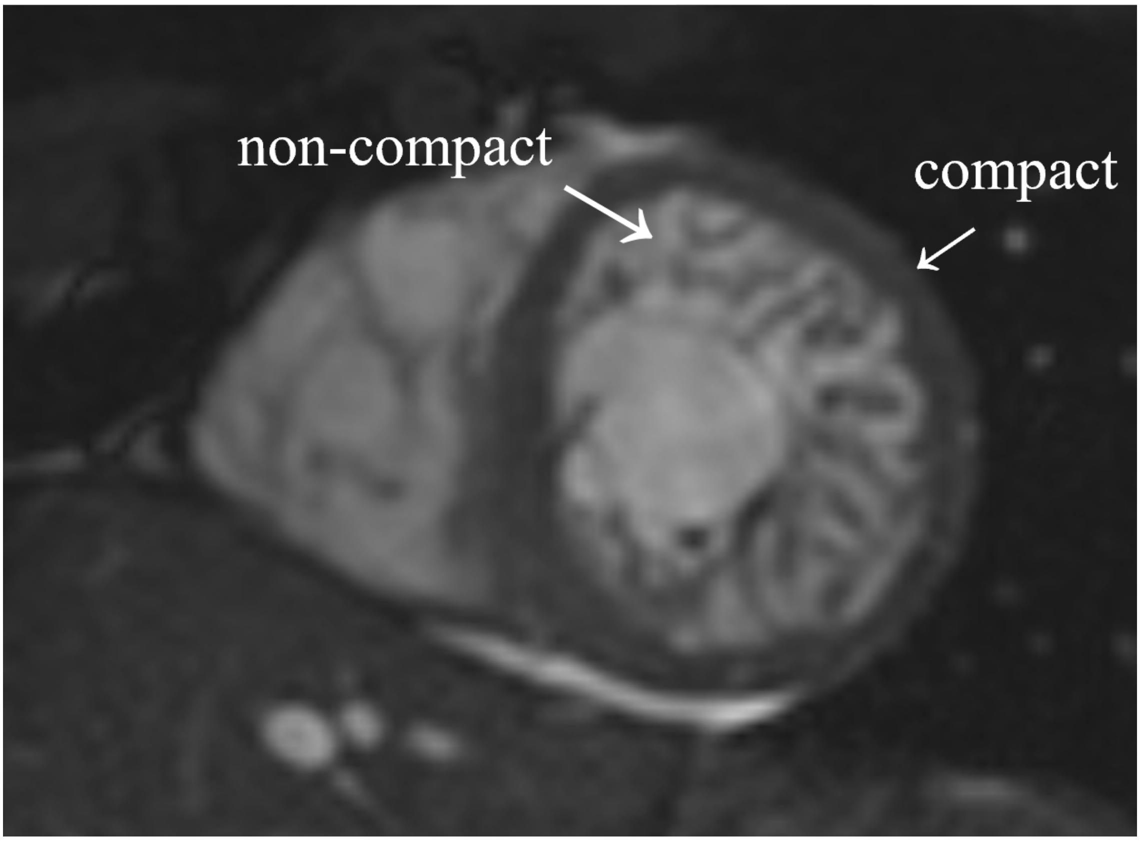

Figure 6. Measurement of the NC and C layers on a CMR SAX image in ED in an LVET subject.

According to the Petersen criterion, when non-compacted to compacted myocardial thickness ratio (NC/C) is greater than 2.3, the diagnosis of LVET can be established. NC: non-compact; C: compact; CMR: cardiac magnetic resonance imaging; SAX: short axis view; ED: end diastole; LVET: left ventricular excessive trabeculation.

Source: Semmelweis University Heart and Vascular Center

For the assessment of LVET, cine steady-state free precession (SSFP) sequences are acquired in standard long-axis views and in contiguous short-axis stacks covering the entire LV. This protocol ensures adequate spatial and temporal resolution for the delineation of myocardial morphology. High blood–myocardium contrast provided by SSFP facilitates recognition of trabeculations, although image quality can be compromised by partial-volume effects, particularly in thin-walled segments and at the apex. A slice thickness of ≤8 mm with no interslice gap is recommended to minimize underestimation of trabecular mass [31].

Image acquisition is followed by dedicated offline analysis, during which endocardial borders are traced on the cine images to delineate the compacted and trabeculated myocardial layers. The precision of this process depends on accurate definition of the endocardial–blood pool interface, which is critical for reproducible quantification of trabecular mass and compact wall thickness. This post-processing step, performed at specialized workstations, is distinct from the scanning session itself and represents a key determinant of measurement reliability and inter-observer agreement.

Accurate endocardial border definition is critical: the contour should follow the compacted myocardium, excluding papillary muscles but including the intertrabecular recesses and the trabecular layer itself [**Figure 7**]. Quantification can be performed manually or semi-automatically using dedicated post-processing platforms such as cvi42 (Circle Cardiovascular Imaging), QMass (Medis), or in research contexts, custom threshold-based (TB) methods, which can help assess intracavitary trabecular mass [32].

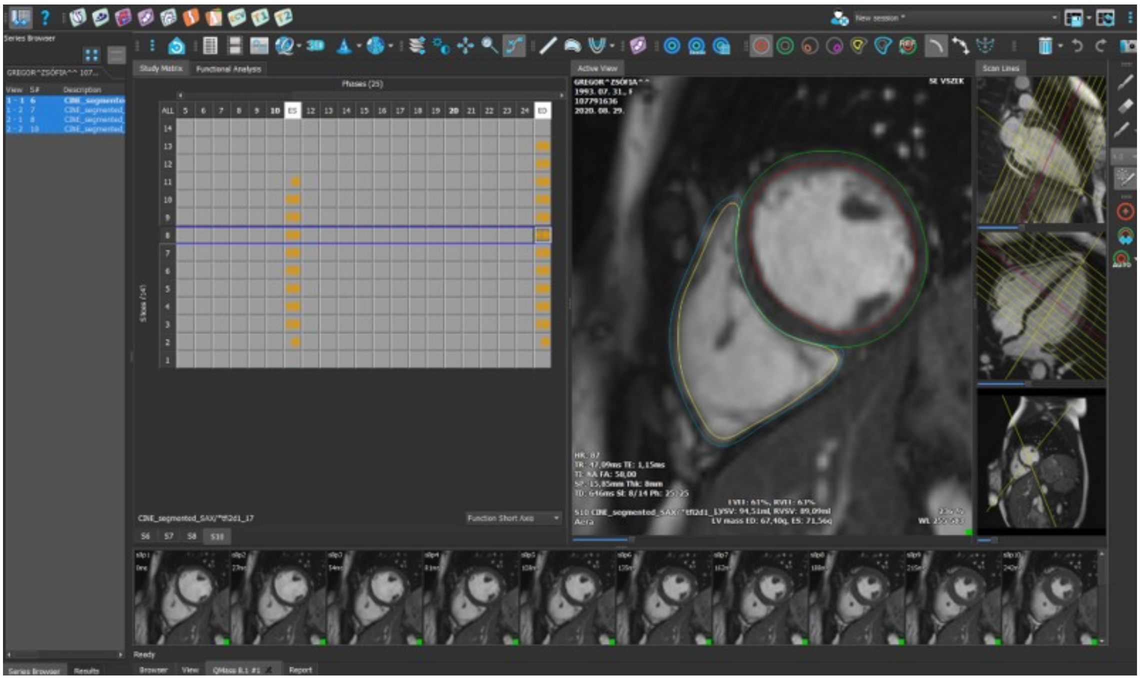

Figure 7. Left ventricular contouring using Medis QMass software.

End-diastolic short-axis CMR image with semiautomatic delineation. The epicardial contour (green) delineates the total myocardial mass, while the endocardial border (red) follows the interface of the trabeculated myocardium and the papillary muscles, thereby enclosing the entire trabeculated myocardial layer within the endocardial contour.

Source: Semmelweis University Heart and Vascular Center

Beyond morphological parameters, CMR also enables detailed functional assessment through feature tracking (FT-CMR), which applies image-based tissue-tracking algorithms to cine images to derive global parameters such as global longitudinal (GLS), global circumferential (GCS), and segmental myocardial strain, strain rate, rotation, and torsion without the need for additional tagging sequences [33]. Dedicated software solutions, such as the QStrain module (Medis Medical Imaging Systems), are commonly employed for FT-CMR analysis [**Figure 8**].

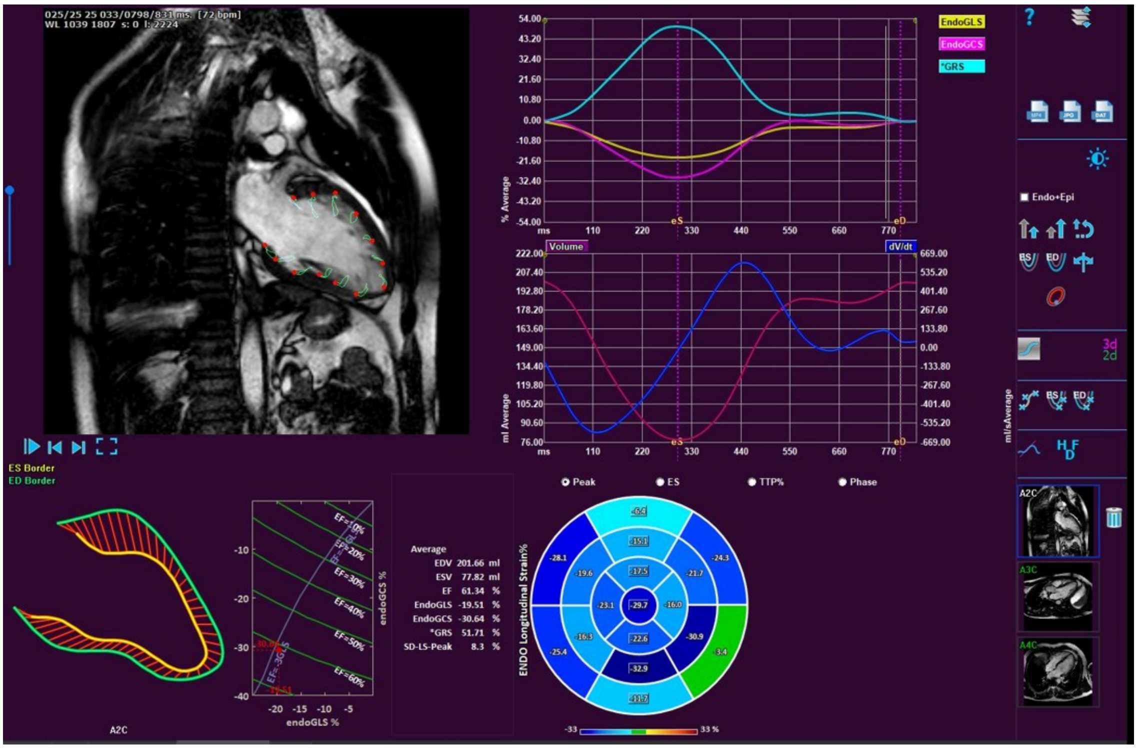

Figure 8. Myocardial strain analysis using Medis Suite feature tracking software. *Cardiac magnetic resonance cine images were post-processed with feature tracking to quantify myocardial deformation. Global strain curves are displayed in longitudinal and circumferential directions, while the bull's-eye plot demonstrates segmental strain distribution.*

Source: Semmelweis University Heart and Vascular Center

FT-CMR is particularly valuable in LVET because it is capable of detecting subtle global and regional dysfunction even when the ejection fraction is preserved. Both left and right ventricular strain abnormalities have been shown to carry independent prognostic value, including in subclinical stages, predicting adverse remodeling, arrhythmic events, and mortality [31].

1.4.2. Echocardiography

Echocardiography remains the first-line imaging modality for detecting myocardial hypertrabeculation due to its availability, real-time imaging, and ability to assess both morphology and hemodynamics. Standard two-dimensional (2D) imaging allows visual identification of excessive trabecular projections and deep intertrabecular recesses, with the Jenni criteria being the most widely applied:

- Bilayered myocardium with an NC/C ratio >2.0 in end-systole [**Figure 9**].
- Colour Doppler evidence of deep intertrabecular recesses filled from the ventricular cavity.
- Absence of coexisting cardiac abnormalities that could account for the findings [34].

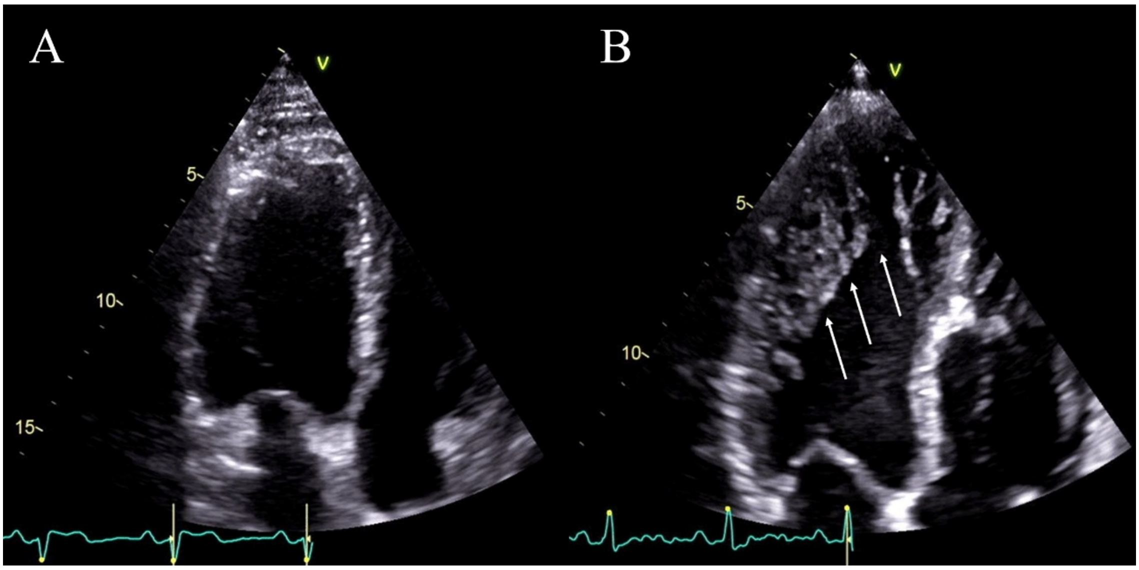

Figure 9. Two dimensional transthoracic echocardiographic images of the left ventricle. The white arrows show the hypertrabeculated myocardium.

A: Healthy subject with normal myocardial architecture.

B: LVET subject with prominent endocardial noncompacted layer.

Source: Semmelweis University Heart and Vascular Center

In addition to 2D imaging, three-dimensional echocardiography (3 TTE) provides full-volume datasets enabling more accurate measurement of ventricular volumes, ejection fraction, with improved agreement with CMR [35].

Modern echocardiography offers advanced speckle tracking techniques, both in 2D and 3D, which enable quantification of myocardial deformation (strain, strain rate) and rotational mechanics [**Figure 10**]. 2D speckle tracking echocardiography (2D-STE) is widely used for GLS measurement, which has proven sensitive for detecting early ventricular dysfunction in LVET [36, 37]. 3D speckle tracking echocardiography (3D-STE) further allows assessment of global circumferential and area strain, offering more comprehensive characterization of myocardial mechanics and reducing geometric assumptions compared with 2D methods [38]. Both LV and RV strain parameters, even when only subtly reduced, have demonstrated prognostic value, being associated with higher rates of heart failure progression, arrhythmias, and adverse outcomes [38, 39].

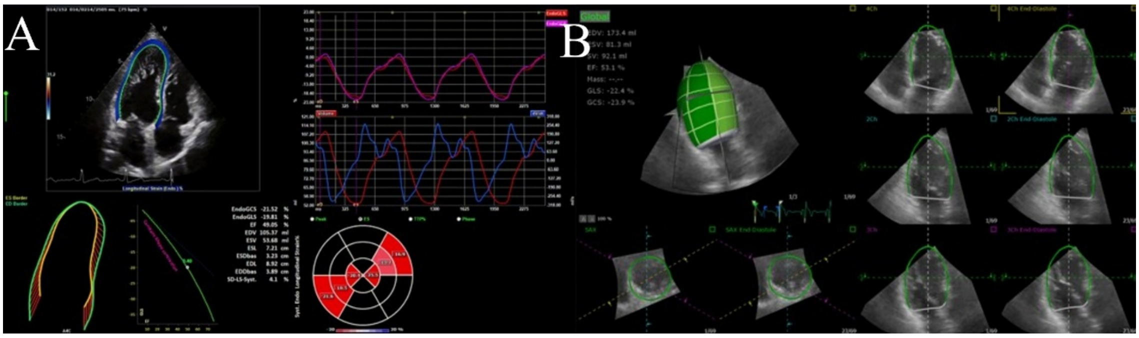

Figure 10. Speckle tracking echocardiography in a subject with LVET.

A: Two-dimensional speckle tracking analysis displaying strain curves and segmental strain bull's-eye plot. TomTec Cardiac Performance analysis

B: Three-dimensional speckle tracking echocardiography with reconstruction of the left ventricle. Semiautomated endocardial contouring providing volumesetric and functional parameters, as well as global strain values. TomTec 4D-LV Analysis

Source: Semmelweis University Heart and Vascular Center

For the RV, echocardiographic diagnosis of hypertrabeculation is inherently more challenging due to its complex geometry and higher physiological trabecular density. There are no universally accepted echocardiographic cut-offs; therefore, evaluation of RV hypertrabeculation relies on a combination of morphological impression, functional indices, and deformation parameters from speckle tracking and 3D_TTE [25, 38] [**Figure 11**]. In this context, multiparametric functional evaluation has prognostic importance, as RV strain impairment, even in the presence of preserved conventional indices, predicts worse outcomes in various cardiomyopathies [38].

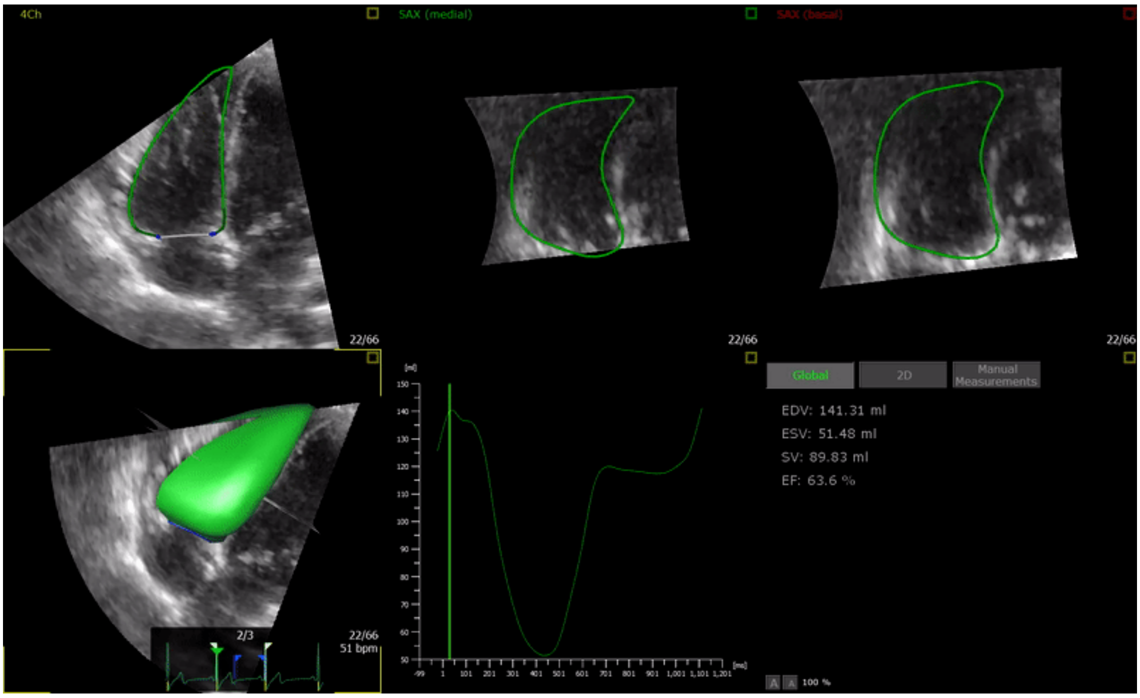

Figure 11. Three-dimensional speckle tracking echocardiography of the right ventricle.

Semiautomatic endocardial contouring of the right ventricle with volumetric reconstruction and deformation analysis. The lower panel displays global volume and strain curves across the cardiac cycle, while calculated volumetric parameters (EDV, ESV, SV, EF) are shown on the right. TomTec 4D RV Function.

Source: Semmelweis University Heart and Vascular Center

Recent advances in three-dimensional echocardiographic post-processing include the ReVISION method, which enables comprehensive assessment of RV mechanics by decomposing myocardial motion into longitudinal, radial, and anteroposterior components [**Figure 12**]. This approach provides a more nuanced description of the complex contraction pattern of the right ventricle than conventional indices, and has been applied in a wide range of pathologies, including pulmonary hypertension, heart failure, and tricuspid regurgitation [40, 41]. By quantifying directional motion and deriving indices such as the longitudinal, radial, and anteroposterior ejection fractions, ReVISION enhances the sensitivity of echocardiography for detecting early or subtle RV dysfunction and may refine prognostic stratification in conditions where standard functional measures may appear preserved [40, 42].

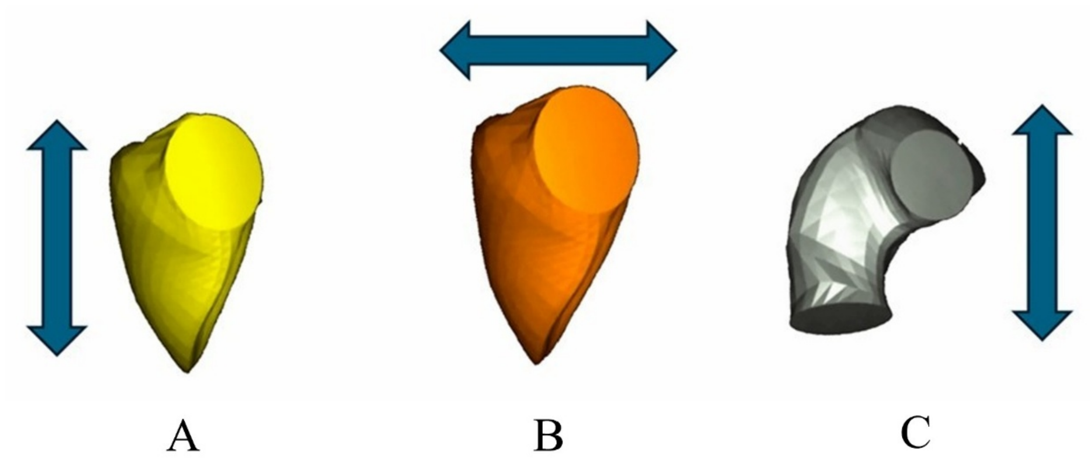

Figure 12. Decomposition of RV motion derived from 3D echocardiography.
Representative 3D RV models illustrating the three orthogonal components of global ejection fraction: (A) longitudinal shortening, (B) radial shortening, and (C) anteroposterior shortening. Arrows indicate the predominant contraction axis in each direction.
Source: Semmelweis University Heart and Vascular Center

Although both CMR and echocardiography have proven utility in the evaluation of myocardial hypertrabeculation, several unresolved issues remain. Existing morphological thresholds were largely developed in small, selected cohorts and may not reliably discriminate between physiological variants and pathological forms of LVET. Inter-modality agreement is imperfect: CMR generally measures thicker non-compacted layers compared with echocardiography, while 3DE and 3D-STE mitigate but do not eliminate these differences. The integration of functional parameters, strain, torsion, and rotational mechanics into routine evaluation shows strong potential to improve risk stratification, but still lacks standardized cut-offs and large-scale validation. Addressing these limitations will require harmonization of imaging protocols, direct head-to-head modality comparisons, and further development of advanced echocardiographic techniques that can combine the accessibility of ultrasound with the reproducibility and spatial resolution of CMR.

1.5. Problem statement

Although advances in cardiac imaging have markedly enhanced the recognition of LVET, its clinical relevance remains debated, particularly in asymptomatic individuals or those with preserved systolic function. With the 2023 ESC cardiomyopathy guidelines no longer designating LVET as an independent cardiomyopathy, comprehensive characterization of both ventricles has become especially pertinent in patients with preserved LV function.

A major challenge remains the consistent evaluation of LVET across different imaging modalities. Although cardiac magnetic resonance (CMR) is the reference standard for morphological characterization, echocardiographic techniques, particularly three-dimensional transthoracic echocardiography (3D TTE), are increasingly advanced and widely used. However, the comparability of CMR and echocardiographic data in this context has not been definitively established, especially for volumetric and functional parameters.

The RV may also be involved in LVET, yet its alterations are often overlooked due to anatomical complexity and higher physiological trabeculation. This intricate morphology makes it difficult to reliably quantify RV volumes and function, and in cases of biventricular involvement, the detection of subclinical RV abnormalities based on imaging is even more challenging.

Conventional functional indices may not fully capture early or regional dysfunction, particularly in the RV. Although emerging analytical tools, such as direction-specific decomposition of RV contraction, can detect subtle mechanical alterations that precede overt dysfunction, this approach has not been systematically investigated in LVET.

Taken together, these considerations underline the pressing need for integrative, multimodal investigations to more precisely characterize the structural and functional features of both ventricles in LVET and establish the diagnostic interchangeability of contemporary imaging modalities. Addressing these gaps forms the rationale for the three studies presented in this dissertation.

2. Objectives

2.1. Comparison of imaging modalities for LVET morphology

Multimodality assessment plays a key role in the evaluation of LVET. Although CMR is often considered the gold standard for characterizing LV structure and function, echocardiographic methods, particularly 2D and 3D TTE, are widely applied due to their accessibility, especially during follow-up. Nevertheless, the level of concordance between these modalities in hypertrabeculated hearts has not been comprehensively defined.

Thus, our first study aimed to compare 2D TTE, 3D TTE, and CMR in the evaluation of LV volumes, ejection fraction, and myocardial strain parameters in individuals with LVET and healthy controls.

2.2. Highlights of right ventricular characteristics of LVET using 3D echocardiography

RV hypertrabeculation often remains unnoticed because of the complex geometry of the chamber and the limitations of 2D imaging. Advanced 3D echocardiography enables a more precise assessment of RV volume and strain, uncovering subtle abnormalities in LVET.

The second study aimed to characterize RV volumes and deformation parameters in LVET subjects using 3D echocardiography. In addition, the relationship between RV and LV parameters were examined to better understand potential biventricular involvement in hypertrabeculated morphology.

2.3. 3D echocardiographic assessment of right ventricular involvement in LVET from a new perspective

In LVET, conventional RV parameters may appear normal, yet specific components of RV wall motion can be selectively altered, changes not captured by standard volumetric or strain measurements.

The third study, therefore, utilized a unique 3D echocardiographic tool to separately quantify these directional wall motion components in individuals with LVET.

3. Methods

3.1. Study design and population

All three studies presented in this dissertation were conducted within the framework of a dedicated LVET registry maintained by our workgroup at the Heart and Vascular Center, Semmelweis University. All patients with CMR-confirmed LVET morpholohy were enrolled in the registry without preselection, allowing comprehensive phenotypic characterization across the full spectrum of this morphological trait. The registry was established with the aim of systematically collecting clinical and multimodal imaging data of all individuals identified with an LVET phenotype, irrespective of clinical presentation, ventricular function, or associated conditions.

From this registry, specific study populations were retrospectively selected for each of the three investigations using uniform and predefined criteria. For all analyses, only patients with preserved left ventricular systolic function were included in order to focus on subtle morphological and functional alterations associated with LVET itself, while minimizing the confounding effects of overt myocardial dysfunction or secondary remodeling. Accordingly, only individuals with a left ventricular ejection fraction greater than 50% were eligible for inclusion in the final study cohorts.

In all patients with CMR-confirmed LVET, the diagnosis fulfilled both the Petersen and the Jacquier criteria.

Using these selection principles, three partially overlapping cohorts were defined. The study comparing imaging modalities for LVET morphology included 38 patients (mean age: 31 ± 14 years; males: n = 19) with preserved LV function and 38 healthy control subjects (mean age: 36 ± 13 years; males: n = 25) matched for age and sex. The investigation focusing on RV characteristics using three-dimensional echocardiography enrolled 41 LVET patients (mean age: 39.58 ± 15 years; males: n = 26) and 41 matched healthy controls (mean age: 39.64 ± 15 years; males: n = 26). The third study, which assessed right ventricular involvement from a novel three-dimensional echocardiographic perspective, analyzed 37 LVET patients (mean age: 40.2 ± 15years; males: n = 22) and 37 matched healthy individuals (mean age: 40.3 ± 15 years; males: n = 22).

Across all three studies, uniform exclusion criteria were applied. Patients were excluded if they had congenital heart disease, documented coronary artery disease or prior myocardial infarction, other cardiomyopathy phenotypes, including dilated, hypertrophic, restrictive, or arrhythmogenic cardiomyopathy, or relevant systemic conditions known to affect myocardial structure or function, such as diabetes mellitus, chronic kidney disease, systemic inflammatory diseases, or neuromuscular disorders. Individuals with uncontrolled arterial- or pulmorary hypertension or a history of high-intensity or competitive physical activity exceeding six hours per week were also excluded. In addition, subjects with suboptimal image quality that precluded reliable segmentation, post-processing, or quantitative analysis were not included.

Healthy control subjects were selected from an institutional healthy control database maintained by our research group and were matched to the patient populations for age and sex. All control participants had no history of cardiovascular or relevant systemic disease and demonstrated normal cardiac morphology with preserved ventricular systolic function on imaging.

This structured, registry-based selection process ensured that all three studies examined well-defined LVET populations with preserved systolic function, enabling focused investigation of morphological characteristics and subtle biventricular functional alterations beyond conventional clinical parameters.

3.2. Image acquisition and analysis

All echocardiographic and magnetic resonance imaging procedures were performed in accordance with the recommendations of the European Society of Cardiology. The imaging protocols and analytic methods varied slightly between the three studies, depending on the specific research focus.

Cardiac magnetic resonance imaging (CMR) was applied exclusively in the first study to allow for a detailed assessment of LV volumes and deformation characteristics. CMR was performed using either a 1.5-T Philips Achieva system (Philips Medical System, Eindhoven, Netherlands) or a Siemens Magnetom Aera scanner (Siemens Healthineers AG, Erlangen, Germany), both equipped with a 5-channel cardiac coil. ECG-gated, balanced steady-state free precession (bSSFP) sequences were acquired in standard 2-, 3-, and 4-chamber long-axis views, as well as in breath-hold short-axis stacks covering the entire LV from base to apex. Imaging parameters included a spatial resolution of 1.5 × 1.5 mm, a temporal resolution of 25 frames per cardiac cycle, a slice thickness of 8 mm with no interslice gap, and a field of view adapted to patient body size (mean 350 mm).

Quantitative CMR analysis was conducted using the QMass module (for volumetric, functional, and myocardial mass assessment) and the QStrain module (for feature-tracking analysis), both integrated into the Medis Suite software (version 3.0; Medis Medical Imaging Systems, Leiden, Netherlands). LV endocardial borders were first automatically generated across all short-axis slices and subsequently manually refined when required, with particular attention to ensuring that the contour encompassed the trabeculated layer within the cavity. Both GLS and GCS were derived from long-axis cine images.

Short-axis (SAX) images were acquired prior to contrast administration to prevent degradation of image quality.

The 2D TTE and 3D TTE were performed in all three studies using a GE Vivid E95 ultrasound system equipped with a 4Vc-D matrix-array transducer (GE Vingmed Ultrasound, Horten, Norway). Standard 2D echocardiographic loops were acquired in the apical long-axis, two-, and four-chamber views with ECG gating and a target frame rate exceeding 50 frames per second.

In the first study, 2D images were analyzed using TOMTEC Cardiac Performance Analysis software (TOMTEC Imaging Systems GmbH, Unterschleissheim, Germany), which enabled semi-automated delineation of LV endocardial borders and speckle tracking-based calculation of volumetric and strain parameters.

For 3D echocardiographic assessment, full-volume LV- and RV-focused datasets were acquired from the apical four-chamber view using multibeat reconstruction across four cardiac cycles. Post-processing was performed using 4D LV Analysis and 4D RV Function software (TOMTEC Imaging Systems GmbH), with automatically generated endocardial contours in both ventricles across all planes and time frames, which were manually adjusted only when necessary. The endocardial border was consistently defined at the interface between compact and noncompacted myocardium to include trabeculations within the cavity. Speckle tracking was employed to derive global deformation parameters.

All echocardiographic analyses were performed by experienced observers. CMR data were independently analyzed by two experts (A.Sz., 9 years; A.R.K., 5 years of experience), while 2D and 3D echocardiographic datasets were evaluated by two observers with 5 and 3 years of experience, respectively (A.Sz. and M.H.) [15]. Interobserver agreement was assessed in a randomly selected subset of LVET patients and healthy controls, which was reanalyzed by a second independent observer blinded to the original measurements and clinical data. Both observers performed complete post-processing and quantitative analyses using identical image datasets and standardized analysis protocols.

3.3. Parameters investigated

Across the three studies included in this dissertation, a predefined core set of left ventricular volumetric and functional parameters was investigated using multimodality imaging. These parameters constituted the common analytical framework of all investigations and included end-diastolic volume (EDV), end-systolic volume (ESV), stroke volume (SV), ejection fraction (EF), global longitudinal strain (GLS), and global circumferential strain (GCS). All volumetric parameters were indexed to body surface area and are reported as indexed values (i) where applicable.

In the study comparing imaging modalities for LVET morphology, this common parameter set was quantified using three different imaging techniques, namely two-dimensional transthoracic echocardiography (2D TTE), three-dimensional transthoracic echocardiography (3D TTE), and cardiac magnetic resonance imaging (CMR), allowing direct intermodality comparison of LV volumetric and deformation parameters.

The investigation focusing on right ventricular characteristics using 3D echocardiography extended the analysis beyond the common LV parameter set by incorporating right ventricular volumetric and functional assessment derived exclusively from 3D TTE. In this study, left- (LV) and right ventricular (RV) EDV, ESV, SV, and EF were evaluated, complemented by deformation analysis of the RV myocardium using septal longitudinal strain (SLS) and free wall longitudinal strain (FWLS). All RV volumetric parameters were indexed to body surface area (i).

The third study further expanded right ventricular assessment by applying advanced motion analysis using dedicated ReVISION software. In addition to conventional RV volumetric and deformation parameters (EDV, ESV, SV, EF), global area strain (GAS) was quantified to provide a more comprehensive evaluation of RV myocardial mechanics. Furthermore, this approach enabled decomposition of RV systolic function into direction-specific components, including longitudinal ejection fraction (LEF), radial ejection fraction (REF), and anteroposterior ejection fraction (AEF). To characterize the relative contribution of each directional component to overall RV performance, the ratios of these parameters to global RV ejection fraction were calculated (LEF/RVEF, REF/RVEF, and AEF/RVEF), allowing detailed characterization of the spatial pattern of right ventricular contraction.

Normal reference values for ventricular volumes, ejection fraction, and myocardial deformation parameters were defined in accordance with contemporary guideline recommendations and large-scale normative. Volumetric parameters were indexed to body surface area and interpreted using sex-specific reference ranges derived from latest echocardiographic and CMR guidelines. Myocardial strain values were interpreted using modality-specific reference ranges and are reported as absolute values.

3.4. Statistical analysis

All statistical analyses were performed using SPSS (IBM, New York, USA), and in the second and third studies, Microsoft Excel (Microsoft, Redmond, USA) was also utilized for supplementary evaluations. Data normality was assessed in each study using the Shapiro–Wilk test. Depending on the distribution of continuous variables, comparisons between groups were carried out using an unpaired two-sided Student's t-test for normally distributed data or the Mann–Whitney U test for non-normally distributed data.

Interobserver agreement for left and right ventricular volumetric, functional, and deformation parameters was assessed using intraclass correlation coefficients (ICCs), calculated with a two-way random-effects model with absolute agreement to account for both systematic and random interobserver differences. ICCs were derived from measurements obtained by independent observers and are reported with corresponding 95% confidence intervals. Agreement was interpreted according to established thresholds: values below 0.50 indicated poor agreement, 0.50–0.75 moderate, 0.75–0.90 good, and values above 0.90 excellent interobserver reliability.

Pearson correlation analysis was used throughout all studies to examine relationships between continuous variables. Correlation strength was classified as weak (<0.3), moderately good (0.3–0.6), or excellent (>0.6), depending on the Pearson correlation coefficient.

Statistical significance was defined by a p-value threshold of <0.05.

Additionally, in the first study, which compared three imaging modalities for LV assessment, the agreement between methods was further explored using Bland–Altman analysis. To quantify intermodality variability, percentage error (PE) was calculated by dividing the limits of agreement by the mean value of the measurements. A PE below 0.3 was considered an acceptable threshold for clinical agreement, in line with previously established methodology.

In the second study, multiple linear regression was also applied to identify independent predictors of right ventricular volumetric parameters.

Across all studies, statistical methods were selected to ensure methodological consistency while also addressing the specific research aims of each investigation.

Given the exploratory nature of the present investigations and the relative rarity of the LVET phenotype, no a priori sample size calculation was performed. Instead, statistical power was assessed post hoc based on the observed effect sizes and the final sample sizes of the individual study cohorts. This approach was considered appropriate, as the primary aim of the studies was detailed morphological and functional characterization using advanced imaging techniques rather than hypothesis-driven outcome prediction. Post hoc analyses indicated an acceptable statistical power for the main volumetric and functional parameters, supporting the robustness of the observed differences between LVET patients and healthy control subjects.

4. Results

The Results section is structured to reflect the sequential design of the three studies, progressing from a multimodality comparison of left ventricular morphology, through a comprehensive biventricular functional assessment using three-dimensional echocardiography, to an advanced, direction-specific analysis of right ventricular mechanics.

For all three studies, a post hoc statistical power analysis based on the observed effect sizes and final cohort sizes indicated an estimated power of approximately 70–75% for the primary volumetric and functional parameters. This level of statistical power was considered acceptable for exploratory imaging analyses and supports the interpretability of the reported results.

4.1. Results of the study “Comparison of imaging modalities for LVET morphology”

Inter-observer agreement

Inter-observer agreement was assessed for LV volume and strain measurements in all imaging modalities used. The evaluation was performed on a subset of ten randomly selected patients with LVET and ten healthy controls [**Table 2**].

Table 2. Interobserver agreement of the first study

Interobserver agreement was rated as weak below 0.4, moderately good between 0.4 and 0.75, and excellent above 0.75.

TTE: Transthoracic echocardiography; CMR: Cardiac Magnetic Resonance Imaging; EDV: End-diastolic volume; ESV: End-systolic volume; SV: Stroke volume; EF: Ejection fraction; GLS: Global longitudinal strain; GCS: Global circumferential strain; (i): indexed to body surface area

	3D_TTE	2D_TTE	CMR
EDV(i)	0.96 (0.80–0.99)	0.67 (0.56–0.73)	0.98 (0.95–0.99)
ESV(i)	0.95 (0.76–0 99)	0.98 (0.81–0. 99)	0.94 (0.84–0 98)
SV(i)	0.89 (0.52–0.98)	0.90 (0.53–0.98)	0.90 (0.75–0.96)
EF	0.65 (0.58–0.92)	0.89 (0.51–0.98)	0.76 (0.40–0.91)
GLS	0.53 (0.48–0.89)	0.93 (0.67–0.98)	0.96 (0.89–0.98)
GCS	0.58 (0.49–0.79)	0.89 (0.52–0.98)	0.96 (0.89–0.98)

Comparison of volumetric parameters

Across all imaging modalities (2D TTE, 3D TTE, and CMR), the LVET group exhibited higher LV volumes compared to healthy controls [**Table 3**].

Table 3. Baseline characteristics of study groups.

*LVET: Left ventricular excessive trabeculation; TTE: Transthoracic echocardiography; CMR: Cardiac Magnetic Resonance Imaging; EDV: End-diastolic volume; ESV: End-systolic volume; SV: Stroke volume; EF: Ejection fraction; GLS: Global longitudinal strain; GCS: Global circumferential strain; (i): Indexed to body surface area; *: p<0.05*

	Healthy			**LVET**			**p value Healthy vs. LVET**		
Number of patients (male)	38 (25)			34 (19)					
Age (years)	36±13			31±14					
	2D_TTE	**3D_TTE**	**CMR**	**2D_TTE**	**3D_TTE**	**CMR**	**2D_TTE**	**3D_TTE**	**CMR**
EDV(i) (ml/m2)	72.1 ±10.4	74.1±16.3	82.5±19.2	77.4±14.2	81.8±17.7	82.9±15.3	**0.005***	**0.05***	0.1
ESV(i) (ml/m2)	30.6±6.3	30.9±6.9	32.8±10.5	36.5±7.3	37.9±8.7	32.6±8.4	**<0.01***	**<0.01***	0.3
SV(i) (ml/m2)	41.5±6.5	43.1±10.1	49.7±1	40.9±7.4	43.8±9.7	50.2±8.5	0.1	0.1	0.09
EF (%)	57.5±5	58.1±3	60.9±5	52.9±3.0	53.6±3	61.3±8	**<0.01***	**<0.01***	0.8
GLS (%)	-21.5±2.9	-20.2±2.5	-23.9±2.3	-20.6±1.8	-28.9±2.9	-21.1±3.1	0.1	0.07	**<0.01***
GCS (%)	-25.9±3.5	-27.1±2.5	-33.8±4.1	-24.7±3.7	-24.6±2.3	-30.1±3.5	0.2	**<0.01***	**<0.01***

Pairwise comparisons between imaging modalities were conducted in LVET and healthy groups to assess consistency in volume measurements.

In healthy individuals, volumetric parameters showed excellent correlations and strong agreement across all modality pairs, as confirmed by Pearson correlation coefficients and Bland–Altman analyses [**Table 4**].

Table 4. Results of the correlation and Bland Altman analysis of the modality pairs in LVNC patients and Healthy volunteers.

*LVNC: Left ventricular non-compaction; TTE: Transthoracic echocardiography; CMR: Cardiac Magnetic Resonance Imaging; EDV: End-diastolic volume; ESV: End-systolic volume; SV: Stroke volume; EF: Ejection fraction; GLS: Global longitudinal strain; GCS: Global circumferential strain; (i): Indexed to body surface area; LOA: Limits of agreement; PE: Percentage error; *: p<0.05*

A) Healthy																	
2D_TTE vs. 3D_TTE						2D_TTE vs. CMR						3D_TTE vs. CMR					
	Correlation		Bland Altman				Correlation		Bland Altman				Corrrelation		Bland Altman		
	r	p<	Bias	LOA	PE (%)		r	p<	Bias	LOA	PE (%)		r	p<	Bias	LOA	PE (%)
EDV(i)	0.71	0.01	-1.978*	22.7	29.65	**EDV(i)**	0.71	0.01	-10.422*	27.4	29.20	**EDV(i)**	0.94	0.01	-8.444*	12.90	15.616
ESV(i)	0.59	0.01	-0.286*	11.6	25.65	**ESV(i)**	0.48	0.01	-2.176	18.2	55.40	**ESV(i)**	0.89	0.01	-1.89*	10.50	29.976
SV(i)	0.69	0.01	-1.692*	14.2	27.90	**SV(i)**	0.63	0.01	-8.246*	15.4	28.90	**SV(i)**	0.88	0.01	-6.555*	9.40	18.967
EF	0.53	0.01	-0.005	0.9	14.78	**EF**	0.01	0.99	-0.033*	0.14	24.00	**EF**	0.23	0.19	-0.028*	0.10	18.137
GLS	0.11	0.55	-1.403*	7.1	35.19	**GLS**	0.34	0.05	2.281*	5.9	24,.90	**GLS**	-0.05	0.76	3.709*	6.90	28.71
GCS	0.48	0.01	1.282*	6.2	22.78	**GCS**	0.29	0.01	8.074*	9.00	26.40	**GCS**	0.12	0.51	6.683*	9.00	26.682
B) LVNC																	
2D_TTE vs. 3D_TTE						2D_TTE vs. CMR						3D_TTE vs. CMR					
	Correlation		Bland Altman				Correlation		Bland Altman				Correlation		Bland Altman		
	r	p<	Bias	LOA	PE (%)		r	p<	Bias	LOA	PE (%)		r	p<	Bias	LOA	PE (%)
EDV(i)	0.73	0.01	-4.341*	23.70	28.95	**EDV(i)**	0.46	0.01	-5.476*	30.1	36.3	**EDV(i)**	0.67	0.01	-1.135	26.5	31.932
ESV(i)	0.70	0.01	-1.426	12.40	32.65	**ESV(i)**	0.21	0.19	3.834	23.00	70.5	**ESV(i)**	0.39	0.02	5.26*	21.5	65.833
SV(i)	0.66	0.01	-2.915*	14.50	33.00	**SV(i)**	0.55	0.01	-9.309*	14.9	29.7	**SV(i)**	0.75	0.01	-6.394*	12.8	25.45
EF	0.05	0.79	-0.007	0.08	14.66	**EF**	-0.06	0.70	-0.084*	0.16	27.2	**EF**	0.23	0.19	-0.077*	0.2	25.015
GLS	0.17	0.29	-1.627*	6.20	32.72	**GLS**	0.39	0.02	0.491	5.8	27.3	**GLS**	0.014	0.93	2.117*	8.4	39.634
GCS	0.12	0.47	-0.068	8.00	32.58	**GCS**	0.19	0.26	5.37	9.1	30.1	**GCS**	0.19	0.26	5.438*	7.5	24.941

In subjects with LVET, EDV and SV showed moderate to high intermodality correlations; however, ESV correlations were weaker, particularly between echocardiographic and CMR measurements. This discrepancy may reflect the limited visualization of endocardial trabeculations during systole in the LVET population.

Percentage error (PE), calculated based on Bland–Altman plots, supported these findings. In particular, measurements obtained using 3D TTE and CMR demonstrated close agreement in volumetric parameters, with correlation coefficients approaching 0.9 and most PE values well below the threshold of 0.3 commonly accepted for clinical interchangeability.

Comparison of functional parameters

Ejection fraction (EF) and myocardial strain values (GLS and GCS) showed lower correlation and agreement across modalities. These discrepancies were more pronounced in the LVET group. The results of Correlations and Bland-Altman analysis are shown in [**Table 5**].

While the number of statistically significant correlations were comparable between the two groups, the strength and reliability of these associations were generally inferior in the LVET population. Agreement across modalities was observed in 89% of comparisons in healthy controls, but it dropped to 38% in the patient group.

Table 5. Summary of the agreement and correlation data.

LVET: left ventricular excessive trabeculation; TTE: transthoracic echocardiography; CMR: cardiac magnetic resonance imaging; A+: acceptable agreement; A-: unacceptable agreement; C+: acceptable correlation; C-: unacceptable correlation; EDV: End-diastolic volume; ESV: End-systolic volume; SV: Stroke volume; EF: Ejection fraction; GLS: Global longitudinal strain; GCS: Global circumferential strain; (i): Indexed to body surface area

	Healthy			**LVNC**		
	2D_TTE-3D_TTE	**2D_TTE-CMR**	**3D_TTE-CMR**	**2D_TTE-3D_TTE**	**2D_TTE-CMR**	**3D_TTE-CMR**
A+, C+	EDV(i), ESV(i), SV(i), EF, GCS	EDV(i), SV(i), GLS	EDV(i), ESV(i), SV(i)	EDV(i)	SV(i), GLS	SV(i)
A-, C+		ESV(i)		ESV(i), SV(i)	EDV(i)	EDV(i), ESV(i)
A+, C-		EF, GCS	EF, GLS(i), GCS(i)	EF	EF,	EF, GCS
A-, C-	GLS			GLS, GCS	ESV(i), GCS	GLS

Finally, we observed a consistent trend in which both 2D TTE and 3D TTE produced lower volumetric values compared to CMR, and 2D TTE measurements were generally lower than those obtained with 3D TTE. Representative correlation and Bland–Altman plots illustrating these findings are presented in the figures [**Figures 13-15**].

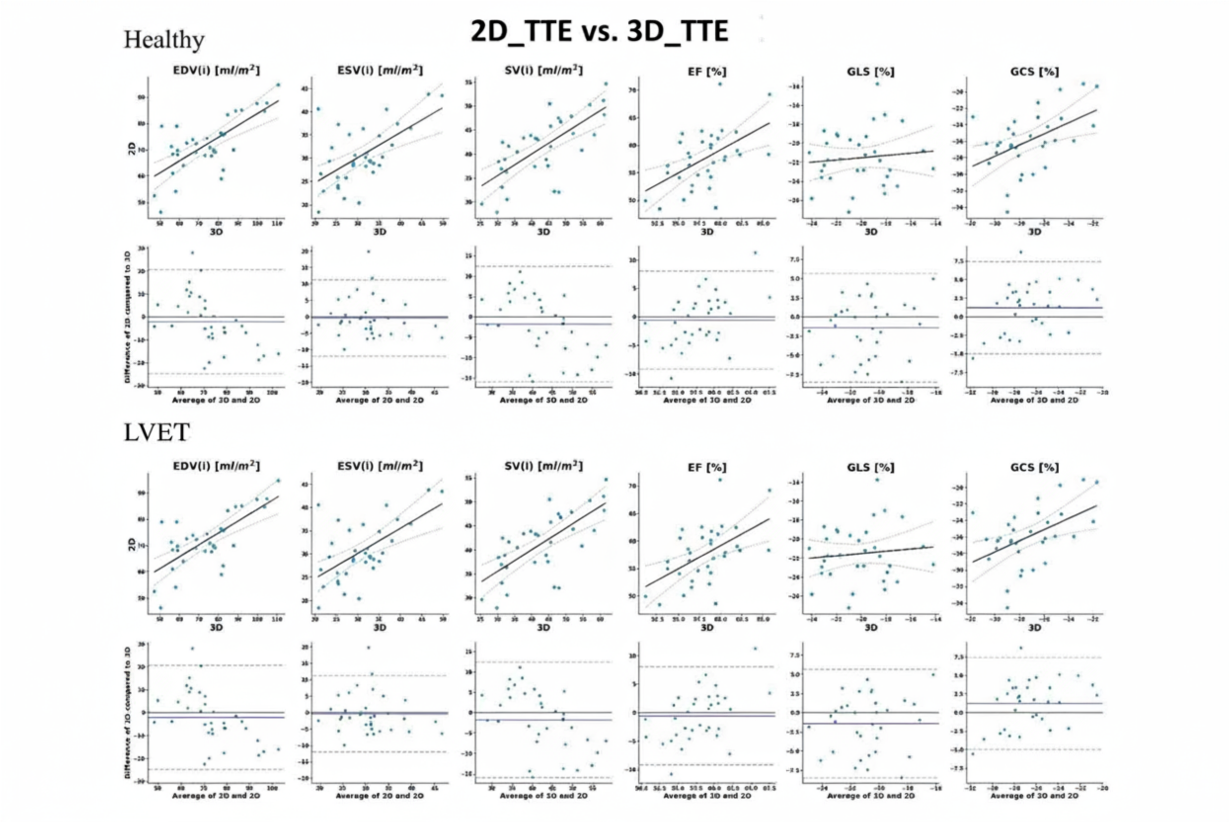

Figure 13. Correlation and Bland Altman plots between 2D echocardiography and 3D echocardiography imaging-derived measurements.

LVET: Left ventricular excessive trabeculation; EDV: End-diastolic volume; ESV: End-systolic volume; SV: Stroke volume; EF: Ejection fraction; GLS: Global longitudinal strain; GCS: Global circumferential strain; (i): Indexed to body surface area

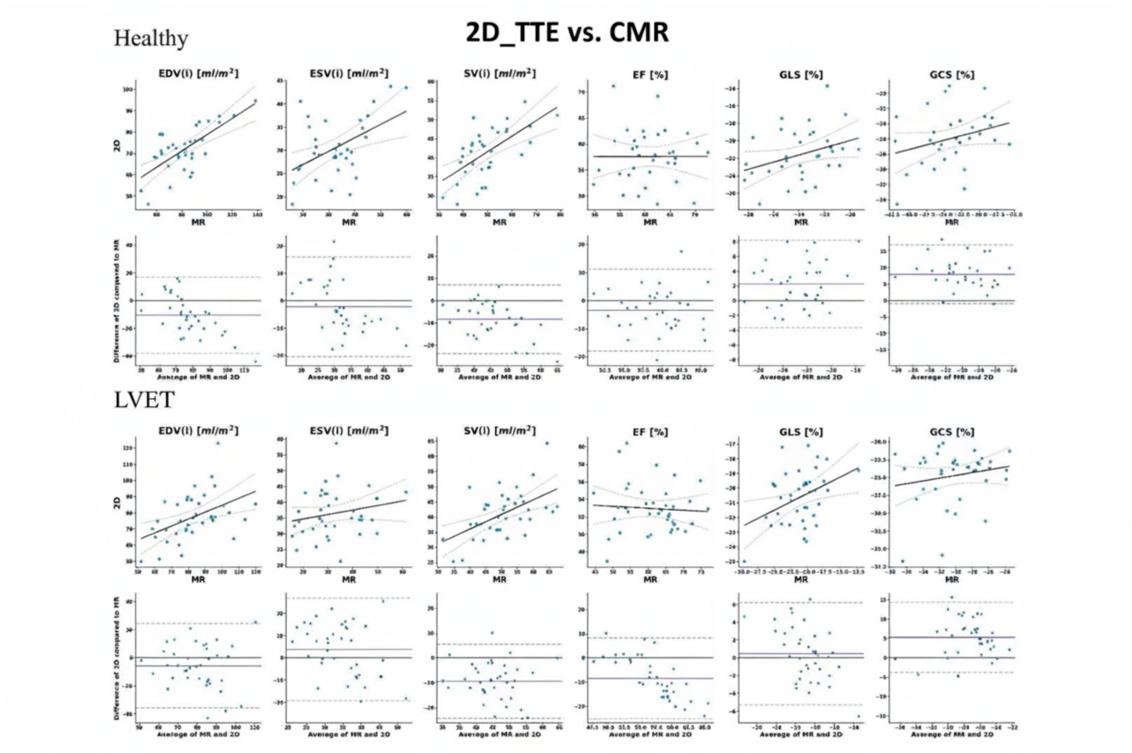

Figure 14. Correlation and Bland Altman plots between 2D echocardiography and CMR imaging-derived measurements.

LVET: Left ventricular excessive trabeculation; EDV: End-diastolic volume; ESV: End-systolic volume; SV: Stroke volume; EF: Ejection fraction; GLS: Global longitudinal strain; GCS: Global circumferential strain; (i): Indexed to body surface area

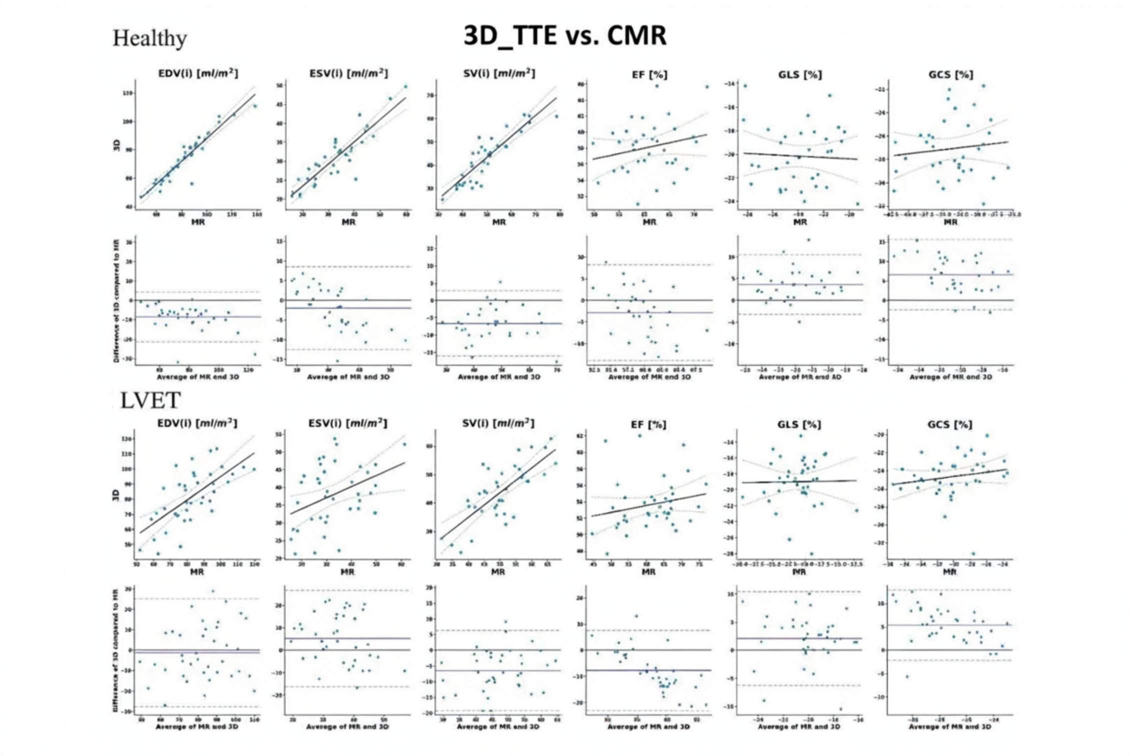

Figure 15. Correlation and Bland Altman plots between 3D echocardiography and CMR imaging-derived measurements.

LVET: Left ventricular excessive trabeculation; EDV: End-diastolic volume; ESV: End-systolic volume; SV: Stroke volume; EF: Ejection fraction; GLS: Global longitudinal strain; GCS: Global circumferential strain; (i): Indexed to body surface area

The following two studies focus on a more advanced three-dimensional echocardiographic assessment of LV and RV structure and function in patients with LVET. Although both study populations were derived from the same registry, they did not fully overlap; therefore, results are presented separately.

4.2. Results of the study "Highlights of right ventricular characteristics of LVET using 3D echocardiography"

Inter-observer agreement

To evaluate measurement reproducibility, inter-observer agreement was assessed for both left and right ventricular measurements using the intraclass correlation coefficient (ICC) in a subset of 10 randomly selected LVET patients and 10 healthy controls [**Table 6**].

Table 6. Interobserver agreement of left and right ventricular parameters in the second and third study

EDV: end-diastolic volume, EF: ejection fraction, GLS: global longitudinal strain, GCS: global circumferential strain, SLS: septal longitudinal strain, FWLS: free-wall longitudinal strain

	LV	RV
EDV(i)	0.98 (0.95-1)	0.96 (0.85-0-99)
EF	0.91 (0.13-0.98)	0.63 (0.58-0.91
GLS	0.92 (0.68-0.98)	
GCS	0.89 (0.19-0.98)	
SLS		0.59 (0.49–0.89)
FWLS		0.56 (0.48–0.89)

Comparison of volumetric and functional parameters

LV volumes in the LVET group remained within normal physiological limits; however, these values were significantly increased in comparison to those observed in healthy subjects. Conversely, functional parameters, including ejection fraction (EF) and myocardial strain (GLS and GCS), were significantly lower in LVET patients compared to controls.

For the right ventricle, volumetric measurements did not differ significantly between LVET subjects and controls. However, similar to the findings of the LV, functional parameters, including RV EF, septal longitudinal strain (SLS), and free wall longitudinal strain (FWLS), were significantly reduced in the LVET group [**Table 7**].

Table 7. Comparison of 3D volumetric and functional parameters of LVET and controls groups.

LVET: left ventricular excessive trabeculation, LV: left ventricular, RV: right ventricular, EDV: end-diastolic volume, ESV: end-systolic volume, SV: stroke volume, EF: ejection fraction, GLS: global longitudinal strain, GCS: global circumferential strain, SLS: septal longitudinal strain, FWLS: free-wall longitudinal strain

LV	LVET	Control	p
EDVi (ml)	76.7 ± 16.6	58.1 ± 9.79	<0.001
ESVi (ml)	36.1 ± 7.9	23.4 ± 4.63	<0.001
SVi (ml)	40.6 ± 9.1	34.9 ± 5.95	<0.001
EF (%)	52.9 ± 2.7	59.8 ± 3.41	<0.001
GLS (%)	-19.0 ± 2.9	-20.6 ± 1.99	<0.001
GCS (%)	-24.1 ± 2.4	-29.9 ± 2.75	<0.001
RV			
EDVi (ml)	56.0 ± 12.0	56.8 ± 12.37	0.854
ESVi (ml)	26.1 ± 6.5	23.9 ± 6.55	0.147
SVi (ml)	30.6 ± 7.3	33.0 ± 6.70	0.095
EF (%)	53.9 ± 5.7	58.8 ± 4.20	<0.001
SLS(%)	-17.5 ± 4.5	-20.6 ± 3.97	<0.001
FWLS (%)	-27.1 ± 5.5	-30.7 ± 5.11	0.006

Biventricular interactions

Further analysis revealed significant biventricular associations. Specifically, RV end-diastolic volume (RV EDV) and stroke volume (RV SV) showed moderate to strong correlations with corresponding LV volumetric parameters. Additionally, RV EF demonstrated a strong linear relationship with both LV EF and LV GLS, whereas RV strain parameters (SLS and FWLS) were significantly associated with LV EF [**Table 8**].

Table 8. Correlation of left and right ventricular parameters in the LVET group.

*LVET: left ventricular excessive trabeculation, LV: left ventricular, RV: right ventricular, EDV: end-diastolic volume, ESV: end-systolic volume, SV: stroke volume, EF: ejection fraction, GLS: global longitudinal strain, GCS: global circumferential strain, SLS: septal longitudinal strain, FWLS: free-wall longitudinal strain, r: correlation coefficient, i: indexed to body surface area, *: p<0.05; **: p<0.01*

		LV_EDVi	LV_ESVi	LV_SVi	LV_EF	LV_GLS	LV_GCS
RV_EDVi	r	0.40*	0.38*	0.40*	0.01	-0.07	-0.05
	p	0.01	0.02	0.01	0.99	0.69	0.79
RV_ESVi	r	0.28	0.34*	0.21	-0.31	-0.32	-0.26
	p	0.09	0.04	0.21	0.06	0.05	0.12
RV_SVi	r	0.42**	0.34*	0.47**	0.26	0.18	0.09
	p	0.01	0.04	0.01	0.12	0.27	0.57
RV_EF	r	016	0.03	0.27	0.55**	0.52**	0.32
	p	0.34	0.89	0.10	0.00	0.01	0.05
RV_SLS	r	-0.05	-0.15	0.04	0.41**	0.22	0.26
	p	0.77	0.37	0.80	0.01	0.18	0.12
RV_FWLS	r	-0.06	-0.19	0.07	0.55**	0.23	0.28
	p	0.74	0.25	0.69	0.000	0.16	0.08

Linear regression analysis was performed to explore these interactions. The results indicated that LV EDV and ESV were significant predictors of right ventricular volumes, suggesting interdependence between the two chambers [**Table 9**].

Table 9. Regression analysis of right ventricular volumetric parameters.

LV: left ventricular, RV: right ventricular, EDV: end-diastolic volume, ESV: end-systolic volume, EF: ejection fraction, GLS: global longitudinal strain, GCS: global circumferential strain, i: indexed to body surface area: p<0,05*

	RV_EDV		RV_ESV	
Covariate	**β**	**p**	**β**	**p**
LV_EDVi	3.855	**0.034***	2.614	**0.036***
LV_ESVi	-7.701	**0.043***	-5.285	**0.044***
LV_EF	-5.075	0.057	-4.006	**0.030***
LV_GLS	-0.661	0.241	-0.624	0.111
LV_GCS	-0.893	0.368	-0.580	0.394
Cumulative r	0.522		0.554	
Standard error	7.805		5.,372	
Cumulative p	**0.025***		**0.014***	

Clinical characteristics

Finally, clinical characteristics of the LVET cohort were also evaluated. More than half of the study participants reported a positive family history of cardiac disease, with a considerable proportion of first-degree relatives diagnosed with inherited myocardial disorders. Notably, 90% of patients had a documented history of arrhythmias. Approximately 12% experienced at least one unexplained syncopal episode of unknown origin. Among those with arrhythmia, ventricular arrhythmias accounted for nearly twothirds of the cases. Furthermore, two individuals required resuscitation during the study period, and one patient suffered a thromboembolic event [**Table 10**].

Table 10. Clinical characteristics of the LVET population.

LVET: left ventricular excessive trabeculation; PM: pacemaker; ICD: implantable cardioverter defibrillator; VES: ventricular extrasystole; NSVT: non-sustained ventricular tachycardia; TIA: transient ischemic attack

Clinical characteristics	Prevalence
Positive family history	51.2%
• Hereditary heart muscle disease	66.7%
• Sudden cardiac death	23.8%
• Arrhythmia	90.5%
• PM / ICD implantation	19.0%
Syncope	12.2%
Arrhythmia confirmed by ECG	39.0%
• Atrial	50.0%
• Ventricular	68.8%
VES	90.9%
NSVT	9.1%
PM implantation	2.4%
Reanimation	4.9%
TIA/Stroke	2.4%

4.3. Results of the study “3D echocardiographic assessment of right ventricular involvement of LVET from a new perspective”

Inter-observer agreement

Measurement reproducibility for both left and right ventricular parameters was assessed in a randomly selected subset of 10 patients with LVET and 10 healthy controls. Intraclass correlation coefficients (ICCs) were calculated to evaluate inter-observer agreement, and detailed results are provided in the Supplementary Material.

Baseline biventricular functional assessment

In the first step of the analysis, conventional volumetric and functional metrics of the left and right ventricles were evaluated. Consistent with the findings of our previous investigations, LVET patients exhibited significantly increased LV volumes compared to controls, while LV_EF and myocardial strain parameters (GLS, GCS) were markedly reduced. Notably, although strain values consistently fell below normal reference thresholds, all other LV parameters remained within the accepted physiological range.

With regard to the right ventricle, volumetric values were generally similar across the two groups, with no statistically significant differences, except for RV EF and the deformation metrics RV GLS and RV GAS, which were significantly lower in the LVET group [**Table 11**].

Table 11. LV and RV volumetric and functional parameters.

LV: left ventricle, RV: right ventricle, EF: ejection fraction, LVET: left ventricular excessive trabeculation, EDV: end-diastolic volume, ESV: end-systolic volume, SV: stroke volume, GLS: global longitudinal strain, GCS: global circumferential strain, GAS: global area strain, (i): indexed to body surface area

LV	**LVET**	**Control**	**p**
EDV(i)	76.3±17.8	58.9±10.2	<0.01
ESV(i)	35.9±8.7	23.6±4.8	<0.01
SV(i)	40.4±96	35.3±6.1	0.008
EF(%)	52.4±3.4	60.1±4.1	<0.01
GLS(%)	-19.1±2.9	-20.6±2.0	0.003
GCS(%)	-24.2±2.6	-30.2±2.7	<0.01
RV	**LVET**	**Control**	**p**
EDV(i)	56.5±13.9	58.1±12.5	0.589
ESV(i)	25.5±7.6	24.2±6.5	0.473
SV(i)	31.0±8.0	33.9±6.8	0.062
EF(%)	55.1±5.6	58.7±4.2	0.003
GCS(%)	-22.4±6.6	-23.3±3.7	0.725
GLS(%)	-19.3±3.1	-22.0±3.3	<0.01
GAS(%)	-37.2±4.5	-40.6±4.0	<0.01

Decomposition-based analysis of RV mechanics and ventricular interactions

To further characterize RV mechanics, we applied a decomposition-based approach using ReVISION software. While LEF and REF were significantly reduced in the LVET population, their absolute values remained within the normal reference range. In contrast, AEF values did not differ significantly between groups.

When analyzing the relative contribution of each directional component to the global RV EF, we observed a significantly higher proportion of AEF in LVET patients, indicating a compensatory shift in the dominant contraction axis. However, the relative shares of LEF and REF contraction were similar between the two groups [**Figure 16-17**].

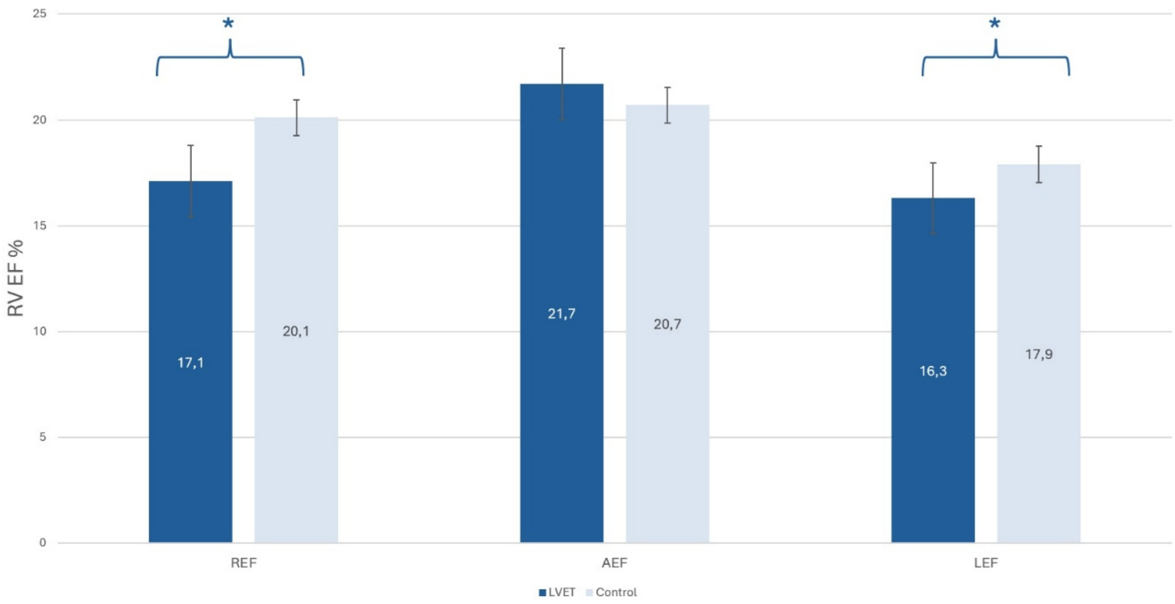

Figure 16. Comparison of 3-way motion components of RV EF.

RV: right ventricle, EF: ejection fraction, , REF: radial ejection fraction, AEF: anteroposterior ejection fraction, LEF: longitudinal ejection fraction

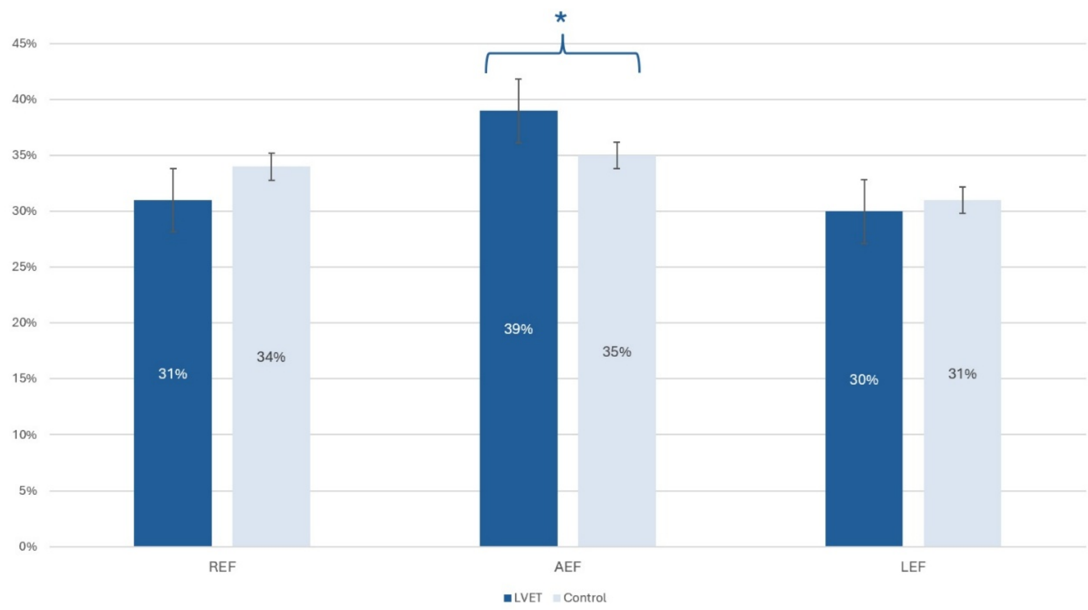

Figure 17. Share of the 3 contraction directions in the global RV EF.

*REF: radial ejection fraction, AEF: anteroposterior ejection fraction, LEF: longitudinal ejection fraction; *: p<0,05*

Correlation analyses revealed moderate to strong associations between left and right ventricular EDV and SV. Moreover, nearly all functional parameters, such as EF and strain values, showed robust positive correlations across the two ventricles [**Table 12**].

Table 12. Correlation of the three contraction directions with LV parameters.

LV: left ventricle, RV: right ventricle, EF: ejection fraction, EDV: end-diastolic volume, ESV: end-systolic volume, SV: stroke volume, GLS: global longitudinal strain, GCS: global circumferential strain, GAS: global area strain, REF: radial ejection fraction, AEF: anteroposterior ejection fraction, LEF: longitudinal ejection fraction

		LV EDV(i)	LV ESV(i)	LV SV(i)	LV EF (%)	LV GLS	LV GCS
REF	r	0.046	0.083	0.011	-0.041	0.059	0.143
AEF	r	0.106	0.068	0.136	0.340*	-0.207	-0.112
LEF	r	0.026	-0.073	0.113	0.234	-0.238	-0.380*

Finally, we investigated the relationships between direction-specific RV contraction components and global LV and RV metrics. While EF was the only LV parameter showing a meaningful association with anteroposterior contraction, most RV parameters demonstrated statistically significant correlations with at least one directional motion component, particularly with AEF [**Table 13**].

Table 13. Correlation of the three contraction directions with RV parameters.

RV: right ventricle, EF: ejection fraction, EDV: end-diastolic volume, ESV: end-systolic volume, SV: stroke volume, GLS: global longitudinal strain, GCS: global circumferential strain, GAS: global area strain, REF: radial ejection fraction, AEF: anteroposterior ejection fraction, LEF: longitudinal ejection fraction

		RV EDV(i)	RV ESV(i)	RV SV(i)	RV EF (%)	RV GLS	RV GCS	RV GAS
REF	r	-0.044	-0.196	0.112	0.357*	-0.498**	-0.043	-0.236
AEF	r	-0.164	-0.412*	0.106	0.340*	0.588**	-0.771**	-0.28
LEF	r	0.023	-0.053	0.09	0.234	0.179	0.571**	-0.431**

5. Discussion

5.1. Discussion of the study “Comparison of imaging modalities for LVET morphology”

Determining the most suitable imaging modality for the follow-up of LVET remains a subject of debate, especially when accurate quantification of volumetric and functional parameters is essential; thus, a critical comparison of these techniques is required.

In our study, we found significant differences in volumetric and functional parameters between LVET patients and healthy individuals across all modalities, which is in line with previous findings [43, 44].

Previous comparative studies addressing LVET are rare. To date, the only relevant intermodality investigation concluded that CMR outperformed 2D TTE in visualizing trabecular structures [45]. However, that study was limited to a single patient group and did not address volumetric or functional measures.

Our study extended this comparison to include both LVET and healthy cohorts and evaluated multiple modalities for volumetric and functional parameters. In healthy subjects, volumetric measures correlated strongly and agreed well across all imaging techniques, suggesting near-interchangeability between 3D TTE and CMR. In contrast, while significant correlations were still observed in the LVET group, the level of agreement among modalities was reduced.

Several other investigations have compared imaging techniques within specific patient group. Hotta et al., for instance, demonstrated strong correlations between 2D and 3D TTE volumetric parameters in patients undergoing cardiac resynchronization therapy, findings that align with our results in both cohorts [46]. However, unlike Hotta et al., we observed limited agreement in ejection fraction (EF) across modalities, except for the 2D vs. 3D TTE comparison in healthy participants. Despite this, percentage errors from Bland–Altman analysis remained within acceptable limits, suggesting that discrepancies were minor. The narrow range of EF values may have limited the detection of significant correlations, especially considering the subtle differences between the groups . This may indicate that the modalities may not be suitable for detecting subtle EF changes in LVET.

An other study also reported moderate to strong correlations between CMR and 2D TTE volumes in heart failure, though their results varied depending on the degree of dysfunction. Similar findings have been published in ischemic heart disease, showing moderate agreement but a systematic underestimation of volumes by 2D TTE relative to CMR [47]. In hypertrophic cardiomyopathy, Bicudo et al. found good volumetric agreement between 2D and 3D TTE; however, EF showed only moderate concordance, with 2D TTE typically underestimating the values [48]. Additionally, Pouleur et al. reported that 3D TTE correlated well with CMR across several patient subgroups, although it tended to underestimate volumes, consistent with our findings in the healthy cohort [49]. Notably, concordance deteriorated in the LVET group. This may reflect the absence of hypertrabeculated pathology in the cohort of Pouleur and the use of contrast-enhanced echocardiography, which likely enhanced endocardial definition and agreement.

Our findings on myocardial strain analysis further emphasize the limitations of intermodality comparisons in LVET. While strain values showed reasonable agreement in healthy participants, LVET patients exhibited poor concordance, with only occasional correlations between feature-tracking CMR and speckle-tracking echocardiography. The poor reproducibility of functional parameters may stem from their limited variability, as previously noted with EF, and from fundamental methodological differences between the techniques. For example, 3D strain is computed from reconstructed surfaces, whereas 2D strain relies on tracking speckles within a single plane.

Pryds et al. evaluated strain using both techniques across various cardiac pathologies and found inconsistent agreement across subgroups, suggesting caution against their interchangeable use [50]. Similarly, Erley et al. reported better intermodality agreement in healthy or ischemic groups but decreased consistency in right ventricular strain analysis in hypertrabeculated cases, underscoring the complexity of using different techniques for deformation analysis [51, 52].

In summary, our study showed excellent intermodality agreement for volumetric data in healthy individuals and acceptable agreement in LVET patients. However, the poor concordance of strain parameters in the LVET group suggests that hypertrabeculation may complicate strain assessment. While echocardiography may serve for follow-up volumetric and functional monitoring after an initial diagnostic CMR, our results caution against the interchangeable use of strain metrics from different modalities in such populations. Further research using more refined techniques is needed to establish modality comparability in diverse pathologies, especially in hypertrabeculated hearts.

As a practical implication, our findings demonstrate that volumetric and functional parameters derived from different imaging modalities are not fully interchangeable in LVET. This represents a novel and clinically relevant observation, particularly in light of the common practice of alternating imaging modalities during follow-up, for example, periodic CMR evaluations complemented by routine echocardiographic assessments.

5.2. Discussion of the study "Highlights of right ventricular characteristics of LVET using 3D echocardiography"

This study utilized 3D echocardiography to assess the morphological and functional characteristics of both ventricles in subjects with primary LVET and preserved systolic function, and compared these findings with those of a healthy control group. In addition, we examined key clinical features of the LVET population.

Although all LV parameters in the LVET group remained within established normal ranges, patients exhibited significantly increased LV volumes and reduced functional parameters, namely LV EF and strain values, compared with healthy controls [53]. These results align with previous CMR investigations involving large LVET cohorts with preserved or mildly reduced LV EF, which similarly demonstrated increased LV volumes and diminished EF and strain metrics when compared to matched controls [26, 35, 54]. Comparable outcomes have also been reported in prior studies using 3D echocardiography, although these were primarily limited to case reports or small-sample studies [55]. To the best of our knowledge, comprehensive 3D echocardiographic analysis of both ventricles in a large LVET cohort had not been previously conducted.

With regard to the RV, all measured values in the LVET group were within normal limits. Although volumes did not differ significantly from those of the control group, RV functional parameters, specifically EF and strain values, were markedly reduced in patients [38]. This observation is consistent with the findings of Sarnecki et al., who applied CMR tissue tracking in a pediatric LVET population and identified diminished RV functional performance. Similarly, Kiss et al. observed decreased RV functional parameters in adult LVET patients on cardiac MRI, although the values also remained within the normal range. However, in contrast to their findings, our study did not identify volumetric differences in the RV, likely due to the smaller sample size.

The concept of ventricular interdependence, whereby the LV contributes significantly to RV function, has been widely recognized, with studies estimating this contribution at 20–40% [56]. Our correlation analysis supports these findings: we observed moderately strong correlations between LV and RV volumetric parameters, as well as a robust association between RV_EF and both LV_EF and LV_GLS, further suggesting right ventricular involvement in LVET.

Notably, a recent investigation by Wang et al., involving 117 LVET patients assessed with 2D speckle-tracking echocardiography (STE), found that impaired RV function, evidenced by reductions in conventional and strain parameters, was an independent predictor of mortality, irrespective of LV function (Wang et al., Carluccio et al.). Building on these findings and our own correlation results, we conducted linear regression analyses, which confirmed that LV volumes significantly predicted RV volumetric and functional parameters. This result suggests that RV involvement may evolve in parallel with LV morphological and functional decline.

Long-term prognostic implications remain debated. A 16-year follow-up study by Vaidya et al. observed reduced survival in a mixed EF LVET population compared to controls; however, no difference in outcomes was noted among those with preserved LV function [57]. Additionally, the MESA study, which followed a cohort of hypertrabeculated patients with preserved EF for nearly a decade, found no significant progression in LV volumes or function over time [58]. These findings are consistent with our clinical observations.

The clinical profile of our patient population was largely benign, which may be attributed to the preserved LV function, as supported by prior studies. Nonetheless, a positive family history and arrhythmic events in a subset of patients highlight the importance of long-term monitoring. Importantly, while most LV parameters remained within normal limits, 3D-derived GLS was slightly reduced, potentially serving as an early marker of functional decline [59, 60].

In summary, while the LVET group demonstrated normal volumetric and functional values, several key parameters were significantly altered compared to healthy individuals, and subtle clinical signs of cardiac involvement were present. These findings underscore the need for longitudinal surveillance in LVET patients with preserved LV function. 3D echocardiography may offer a valuable imaging modality for such monitoring.

5.3. Discussion of the study "3D echocardiographic assessment of right ventricular involvement of LVET from a new perspective"

In this study, three-dimensional echocardiography was applied to characterize both left and right ventricular morphology and function in patients with LVET who had preserved LV_EF, with a particular focus on the complex three-dimensional contraction pattern of the RV, and results were compared with those from healthy controls.

For the LV, our observations are consistent with previous cardiac magnetic resonance (CMR) and echocardiographic studies, which reported increased ventricular volumes and reduced functional indices in LVET compared to controls [53]. In assessing RV involvement, our findings agree with earlier three-dimensional transthoracic echocardiographic data from our group, which also identified moderately impaired RV function in this patient population [26]. CMR studies have similarly described subclinical RV changes in LVET, including larger volumetric indices and reductions in EF and strain, in patients with both preserved and reduced LV EF [35, 54]. Interestingly, Stämpfli et al. concluded that quantifying RV trabeculation does not help to distinguish LVET from healthy hearts, underscoring the clinical importance of focusing on functional assessment [61].

The prognostic relevance of RV dysfunction is well established in multiple cardiovascular conditions [56, 62, 63]. In a cohort of 117 patients with LVET, Wang et al. demonstrated that RV dysfunction predicted all-cause mortality independently of LV function, and impaired RV global longitudinal strain (GLS) was also an independent predictor of adverse outcomes. These findings highlight the importance of routine quantitative RV evaluation in LVET [64].

The advantage of three-dimensional echocardiography is that it comprehensively characterizes RV function by quantifying its distinct contraction components. In our cohort, RV performance in the LVET group appeared to depend primarily on augmented

AEF compared with controls. In contrast, Surkova et al. and Kovács et al. reported that in patients with reduced LV EF of various etiologies, both LEF and AEF shortening components were reduced, with compensatory increases in radial ejection fraction (REF) to maintain overall RV EF [42, 65]. This mechanism may explain the slightly reduced but still normal RV EF observed in our prior CMR study of LVET patients with reduced LV EF [54].

In healthy individuals, the three RV contraction components contribute to the process in a balanced manner [40]. This study also showed that REF compensation predominates in patients with reduced LV function , with early declines in LEF and AEF, a finding corroborated by other large case–control analyses [41, 42]. Conversely, in conditions with elevated RV strain, such as pulmonary embolism or atrial septal defect, longitudinal compensation can dominate irrespective of LV status [40]. Tokodi et al. also demonstrated that in patients undergoing mitral valve replacement, RV motion was LEF-dominant preoperatively, shifted to REF-dominance immediately postoperatively, and returned to a near-normal REF/RV EF ratio by three months [41]. This suggests the potential prognostic value of preoperative three-dimensional RV parameters for predicting postoperative dysfunction.

Notably, among patients with normal RV EF, AEF has emerged as an independent predictor of adverse events [41]. In our study, normal AEF values may indicate a favorable prognosis in LVET patients with preserved LV EF. Furthermore, Gregor et al. observed that global RV function in LVET remains preserved regardless of LV EF status, suggesting a more sustained RV compensatory capacity in this disease than in other cardiomyopathies [66].

In summary, the AEF-predominant RV contraction pattern identified here has not previously been described in LVET and differs from patterns reported in other cardiac diseases, suggesting a possible disease-specific signature. Based on current evidence and our results, analysis of RV contraction components could help detect subclinical dysfunction even when RV EF remains preserved. Further studies with larger cohorts are warranted to confirm these findings and determine whether AEF has prognostic significance in this population.

Limitation

One major limitation of our research is the relatively small sample size, which reflects the rarity of LVET as a condition. Although our registry is continuously expanding, the geographically dispersed nature of the patient population poses significant challenges to conducting prospective, multimodal studies. Additionally, the retrospective design and the lack of longitudinal follow-up data limit the comprehensive assessment of clinical outcomes and the prognostic implications of our findings.

Methodologically, a notable constraint arises from the inherent differences between imaging modalities. Although 2D speckle-tracking echocardiography (2D-STE) and feature-tracking CMR (FT-CMR) provide strain measurements derived from similar approaches, 3D speckle-tracking echocardiography (3D-STE) is based on reconstructed surfaces, complicating direct numerical comparisons across techniques. Furthermore, the inclusion of only patients with preserved left ventricular function resulted in limited variability and small standard deviations in parameters such as EF, GLS, and GCS, potentially reducing the robustness of correlation analyses.

Another important limitation is the lack of external validation in independent cohorts or multicenter studies, which would be necessary to generalize the findings to broader populations. Although intra- and inter-observer variability were assessed, the reproducibility of RV trabecular assessment remains a challenge, particularly given the complex geometry of the chamber and the absence of standardized morphological thresholds. In addition, our studies did not include systematic tissue characterization with CMR (e.g., late gadolinium enhancement or mapping), which could have provided complementary prognostic insights.

Finally, the cross-sectional nature of our analyses precludes definitive conclusions about the temporal evolution of biventricular changes in LVET. Longitudinal imaging studies with clinical follow-up are needed to determine whether the subclinical abnormalities we identified, particularly in RV mechanics, have prognostic relevance or represent adaptive remodeling without adverse outcomes.

6. Conclusion

This doctoral work investigated LVET with preserved systolic function using advanced imaging methods across three consecutive studies. Together, these investigations provided a stepwise characterization of the morphological and functional alterations associated with LVET, with a particular focus on methodological accuracy, biventricular involvement, and RV mechanics.

The first study addressed a core methodological question, whether 2D and 3D TTE provide results comparable to those of CMR, the current gold standard. In healthy individuals, volumetric parameters showed excellent correlation and good agreement across all three modalities. In contrast, subjects with LVET exhibited reduced agreement, particularly for end-systolic volumes, and weaker correlations for deformation metrics. Both 2D and 3D TTE tended to underestimate volumes compared to CMR, highlighting that while 3D TTE approximates CMR more closely than 2D, the complex trabecular morphology limits interchangeability between methods. These findings underscore the need for careful selection of modality and standardized protocols in this group.

The second study shifted its focus to the biventricular profile of LVET using 3D TTE. Although LV volumes were elevated and functional parameters were decreased, all values except strain remained within normal limits. On the RV side, volumes were not significantly different, yet strain and EF were markedly reduced in the LVET group. Strong correlations were observed between LV and RV parameters, and regression analyses confirmed that LV volumes independently predicted RV size. In addition, the study documented relevant clinical features in the LVET cohort, including high arrhythmia burden and familial clustering of myocardial diseases. These findings indicate that right ventricular involvement in LVET, although frequently subclinical, may have functional significance and prognostic implications, underscoring the importance of its recognition as a potential avenue for earlier therapeutic intervention.

Finally, the third study examined RV contraction patterns in detail. While global RV parameters confirmed the previous findings of mildly reduced function, the direction-specific analysis revealed a disproportionate contribution of AEF in subjects with LVET. In contrast, LEF and REF components were reduced but still within normal ranges. Notably, the relative increase in AEF suggests a potential compensatory mechanism, preserving global RV output in the presence of subclinical dysfunction. Correlation analyses further revealed strong interdependence between LV and RV functional parameters and identified distinct associations between specific RV motion components and global ventricular performance.

Taken together, these results highlight the value of 3D imaging in quantifying subtle alterations in chamber size and function. They also demonstrate that RV involvement, although not always apparent in conventional assessments, may play a significant role in the disease phenotype. These insights may support earlier detection, enable individualized monitoring, and inform future risk stratification in this unique population

7. Summary

Primary LVET is a distinct myocardial phenotype marked by excessive trabeculation and deep recesses. Although common in imaging, especially with advanced techniques, its clinical significance in patients with preserved LV function remains unclear. This thesis aimed to characterize LVET based on multimodal imaging, focusing on biventricular function and RV mechanics, through three interrelated studies.

The first compared 2D and 3D transthoracic echocardiography (TTE) with cardiac magnetic resonance (CMR) in LVET patients and controls. Although agreement was good in healthy subjects, there was variability in LVET, especially for end-systolic volumes and strain. This underscores imaging challenges and highlights 3D TTE as superior to 2D in approximating CMR.

The second assessed biventricular parameters with 3D TTE. LV volumes were increased but mostly within normal limits; strain and ejection fraction were reduced. RV volumes appeared preserved, yet deformation and ejection fraction were impaired, indicating subclinical involvement. Strong LV–RV correlations were observed, with LV volumes predicting RV size and performance. Arrhythmias and family history of cardiomyopathy were frequent, suggesting the prognostic importance of RV assessment.

The third used advanced post-processing to analyze RV ejection components: longitudinal and radial contributions were reduced, while anteroposterior motion played a larger role versus controls. This altered pattern may reflect an adaptive mechanism to maintain RV output.

In summary, LVET with preserved systolic function shows consistent subclinical alterations in both ventricles. Comprehensive 3D imaging and advanced analyses were crucial in detecting these changes, emphasizing that this phenotype may not be functionally benign.

8. References

1. Pinto, A.R., A. Ilinykh, M.J. Ivey, J.T. Kuwabara, M.L. D'Antoni, R. Debuque, A. Chandran, L. Wang, K. Arora, N.A. Rosenthal, et al., *Revisiting Cardiac Cellular Composition.* Circ Res, 2016. **118**(3): p. 400-9.
2. Bers, D.M., *Cardiac excitation–contraction coupling.* Nature, 2002. **415**(6868): p. 198-205.
3. Severs, N.J., *The cardiac gap junction and intercalated disc.* International Journal of Cardiology, 1990. **26**(2): p. 137-173.
4. Neff, L.S. and A.D. Bradshaw, *Cross your heart? Collagen cross-links in cardiac health and disease.* Cellular Signalling, 2021. **79**: p. 109889.
5. Gutterman, D.D., D.S. Chabowski, A.O. Kadlec, M.J. Durand, J.K. Freed, K. Ait-Aissa, and A.M. Beyer, *The Human Microcirculation: Regulation of Flow and Beyond.* Circ Res, 2016. **118**(1): p. 157-72.
6. Wu, B., Z. Zhang, W. Lui, X. Chen, Y. Wang, A.A. Chamberlain, R.A. Moreno-Rodriguez, R.R. Markwald, B.P. O'Rourke, D.J. Sharp, et al., *Endocardial cells form the coronary arteries by angiogenesis through myocardial-endocardial VEGF signaling.* Cell, 2012. **151**(5): p. 1083-96.
7. Young, A.A. and B.R. Cowan, *Evaluation of left ventricular torsion by cardiovascular magnetic resonance.* J Cardiovasc Magn Reson, 2012. **14**(1): p. 49.
8. Wilson, A.J., G.B. Sands, I.J. LeGrice, A.A. Young, and D.B. Ennis, *Myocardial mesostructure and mesofunction.* Am J Physiol Heart Circ Physiol, 2022. **323**(2): p. H257-h275.
9. Ahmad, A., H. Li, Y. Zhang, J. Liu, Y. Gao, M. Qian, Y. Lin, L. Yi, L. Zhang, Y. Li, et al., *Three-Dimensional Echocardiography Assessment of Right Ventricular Volumes and Function: Technological Perspective and Clinical Application.* Diagnostics (Basel), 2022. **12**(4).
10. Saremi, F., S.Y. Ho, J.A. Cabrera, and D.n. S??nchez-Quintana, *Right Ventricular Outflow Tract Imaging With CT and MRI: Part 1, Morphology.* American Journal of Roentgenology, 2013. **200**(1): p. W39-W50.

11. González-Casal, D., D. Sánchez-Quintana, A. Jiménez Restrepo, T. Datino, V. Martínez de Vega, S. Bayona Horta, A. Fontela, B. Terol Espinosa de Los Monteros, S. Hernández Jiménez, and J. Cabrera, *The Right Ventricular Moderator Band: From Leonardo da Vinci's Drawings to Current Cardiac Imaging.* JACC Case Rep, 2024. **29**(21): p. 102647.
12. Captur, G., R. Wilson, M.F. Bennett, G. Luxán, A. Nasis, J.L. de la Pompa, J.C. Moon, and T.J. Mohun, *Morphogenesis of myocardial trabeculae in the mouse embryo.* Journal of Anatomy, 2016. **229**(2): p. 314-325.
13. Arbelo, E., A. Protonotarios, J.R. Gimeno, E. Arbustini, R. Barriales-Villa, C. Basso, C.R. Bezzina, E. Biagini, N.A. Blom, R.A. de Boer, et al., *2023 ESC Guidelines for the management of cardiomyopathies: Developed by the task force on the management of cardiomyopathies of the European Society of Cardiology (ESC).* European Heart Journal, 2023. **44**(37): p. 3503-3626.
14. Sedmera, D., T. Pexieder, M. Vuillemin, R.P. Thompson, and R.H. Anderson, *Developmental patterning of the myocardium.* Anat Rec, 2000. **258**(4): p. 319-37.
15. Kawel, N., M. Nacif, A.E. Arai, A.S. Gomes, W.G. Hundley, W.C. Johnson, M.R. Prince, R.B. Stacey, J.A. Lima, and D.A. Bluemke, *Trabeculated (noncompacted) and compact myocardium in adults: the multi-ethnic study of atherosclerosis.* Circ Cardiovasc Imaging, 2012. **5**(3): p. 357-66.
16. Petersen, S.E., J.B. Selvanayagam, F. Wiesmann, M.D. Robson, J.M. Francis, R.H. Anderson, H. Watkins, and S. Neubauer, *Left ventricular non-compaction: insights from cardiovascular magnetic resonance imaging.* J Am Coll Cardiol, 2005. **46**(1): p. 101-5.
17. Petersen, S.E., B. Jensen, N. Aung, M.G. Friedrich, C.J. McMahon, S.A. Mohiddin, R.H. Pignatelli, F. Ricci, R.H. Anderson, and D.A. Bluemke, *Excessive Trabeculation of the Left Ventricle: JACC: Cardiovascular Imaging Expert Panel Paper.* JACC Cardiovasc Imaging, 2023. **16**(3): p. 408-425.
18. Kawel-Boehm, N., R.L. McClelland, F. Zemrak, G. Captur, W.G. Hundley, C.Y. Liu, J.C. Moon, S.E. Petersen, B. Ambale-Venkatesh, J.A.C. Lima, et al., *Hypertrabeculated Left Ventricular Myocardium in Relationship to Myocardial Function and Fibrosis: The Multi-Ethnic Study of Atherosclerosis.* Radiology, 2017. **284**(3): p. 667-675.

19. Towbin, J.A., A. Lorts, and J.L. Jefferies, *Left ventricular non-compaction cardiomyopathy.* Lancet, 2015. **386**(9995): p. 813-25.
20. Petersen, S.E., B. Jensen, N. Aung, M.G. Friedrich, C.J. McMahon, S.A. Mohiddin, R.H. Pignatelli, F. Ricci, R.H. Anderson, and D.A. Bluemke, *Excessive Trabeculation of the Left Ventricle.* JACC: Cardiovascular Imaging, 2023. **16**(3): p. 408-425.
21. Sedaghat-Hamedani, F., J. Haas, F. Zhu, C. Geier, E. Kayvanpour, M. Liss, A. Lai, K. Frese, R. Pribe-Wolferts, A. Amr, et al., *Clinical genetics and outcome of left ventricular non-compaction cardiomyopathy.* Eur Heart J, 2017. **38**(46): p. 3449-3460.
22. Gati, S., M. Papadakis, N.D. Papamichael, A. Zaidi, N. Sheikh, M. Reed, R. Sharma, B. Thilaganathan, and S. Sharma, *Reversible de novo left ventricular trabeculations in pregnant women: implications for the diagnosis of left ventricular noncompaction in low-risk populations.* Circulation, 2014. **130**(6): p. 475-83.
23. Abela, M. and A. D'Silva, *Left Ventricular Trabeculations in Athletes: Epiphenomenon or Phenotype of Disease?* Curr Treat Options Cardiovasc Med, 2018. **20**(12): p. 100.
24. Muresian, H., *The clinical anatomy of the right ventricle.* Clin Anat, 2016. **29**(3): p. 380-98.
25. Addetia, K., F. Maffessanti, D. Muraru, A. Singh, E. Surkova, V. Mor-Avi, L.P. Badano, and R.M. Lang, *Morphologic Analysis of the Normal Right Ventricle Using Three-Dimensional Echocardiography-Derived Curvature Indices.* J Am Soc Echocardiogr, 2018. **31**(5): p. 614-623.
26. Kiss, A.R., Z. Gregor, A. Popovics, K. Grebur, L.E. Szabó, Z. Dohy, A. Kovács, B.K. Lakatos, B. Merkely, H. Vágó, et al., *Impact of Right Ventricular Trabeculation on Right Ventricular Function in Patients With Left Ventricular Non-compaction Phenotype.* Front Cardiovasc Med, 2022. **9**: p. 843952.
27. Vergani, V., D. Lazzeroni, and G. Peretto, *Bridging the gap between hypertrabeculation phenotype, noncompaction phenotype and left ventricular noncompaction cardiomyopathy.* J Cardiovasc Med (Hagerstown), 2020. **21**(3): p. 192-199.

28. Grebur, K., B. Mester, M. Horváth, K. Farkas-Sütő, Z. Gregor, A.R. Kiss, A. Tóth, A. Kovács, A. Fábián, B.K. Lakatos, et al., *The effect of excessive trabeculation on cardiac rotation-A multimodal imaging study.* PLoS One, 2024. **19**(9): p. e0308035.
29. Xu, J., W. Yang, S. Zhao, and M. Lu, *State-of-the-art myocardial strain by CMR feature tracking: clinical applications and future perspectives.* Eur Radiol, 2022. **32**(8): p. 5424-5435.
30. Jacquier, A., F. Thuny, B. Jop, R. Giorgi, F. Cohen, J.-Y. Gaubert, V. Vidal, J.M. Bartoli, G. Habib, and G. Moulin, *Measurement of trabeculated left ventricular mass using cardiac magnetic resonance imaging in the diagnosis of left ventricular non-compaction†.* European Heart Journal, 2010. **31**(9): p. 1098-1104.
31. Grothoff, M., M. Pachowsky, J. Hoffmann, M. Posch, S. Klaassen, L. Lehmkuhl, and M. Gutberlet, *Value of cardiovascular MR in diagnosing left ventricular non-compaction cardiomyopathy and in discriminating between other cardiomyopathies.* Eur Radiol, 2012. **22**(12): p. 2699-709.
32. Gregor, Z., A.R. Kiss, K. Grebur, L.E. Szabó, B. Merkely, H. Vágó, and A. Szűcs, *MR -specific characteristics of left ventricular noncompaction and dilated cardiomyopathy.* Int J Cardiol, 2022. **359**: p. 69-75.
33. Fischer, K., S.J. Obrist, S.A. Erne, A.W. Stark, M. Marggraf, K. Kaneko, D.P. Guensch, A.T. Huber, S. Greulich, A. Aghayev, et al., *Feature Tracking Myocardial Strain Incrementally Improves Prognostication in Myocarditis Beyond Traditional CMR Imaging Features.* JACC Cardiovasc Imaging, 2020. **13**(9): p. 1891-1901.
34. Jenni, R., E. Oechslin, J. Schneider, C. Attenhofer Jost, and P.A. Kaufmann, *Echocardiographic and pathoanatomical characteristics of isolated left ventricular non-compaction: a step towards classification as a distinct cardiomyopathy.* Heart, 2001. **86**(6): p. 666-71.
35. Zhang, J., M. Jiang, C. Zheng, H. Liu, Y. Guo, X. Xie, Z. Zou, X. Zhou, L. Xia, M. Luo, et al., *Evaluation of isolated left ventricular noncompaction using cardiac magnetic resonance tissue tracking in global, regional and layer-specific strains.* Scientific Reports, 2021. **11**(1): p. 7183.

36. van der Bijl, P., M. Bootsma, Y.L. Hiemstra, N. Ajmone Marsan, J.J. Bax, and V. Delgado, *Left ventricular 2D speckle tracking echocardiography for detection of systolic dysfunction in genetic, dilated cardiomyopathies.* Eur Heart J Cardiovasc Imaging, 2019. **20**(6): p. 694-699.

37. Cimino, S., E. Canali, V. Petronilli, F. Cicogna, L. De Luca, M. Francone, G. Sardella, C. Iacoboni, and L. Agati, *Global and regional longitudinal strain assessed by two-dimensional speckle tracking echocardiography identifies early myocardial dysfunction and transmural extent of myocardial scar in patients with acute ST elevation myocardial infarction and relatively preserved LV function.* Eur Heart J Cardiovasc Imaging, 2013. **14**(8): p. 805-11.

38. Muraru, D., A. Niero, H. Rodriguez-Zanella, D. Cherata, and L. Badano, *Three-dimensional speckle-tracking echocardiography: benefits and limitations of integrating myocardial mechanics with three-dimensional imaging.* Cardiovasc Diagn Ther, 2018. **8**(1): p. 101-117.

39. Pastore, M.C., L. Fusini, G.E. Mandoli, C. Carrucola, M. Vigna, M. Muratori, M. Pepi, L. Cavigli, F. D'Ascenzi, M. Focardi, et al., *Prognostic value of left and right ventricular strain in heart failure with reduced and preserved ejection fraction: a meta-analysis.* European Heart Journal, 2022. **43**(Supplement_2): p. ehac544.075.

40. Lakatos, B.K., Y. Nabeshima, M. Tokodi, Y. Nagata, Z. Tősér, K. Otani, T. Kitano, A. Fábián, A. Ujvári, A.M. Boros, et al., *Importance of Nonlongitudinal Motion Components in Right Ventricular Function: Three-Dimensional Echocardiographic Study in Healthy Volunteers.* J Am Soc Echocardiogr, 2020. **33**(8): p. 995-1005.e1.

41. Tokodi, M., E. Németh, B.K. Lakatos, E. Kispál, Z. Tősér, L. Staub, K. Rácz, Á. Soltész, S. Szigeti, T. Varga, et al., *Right ventricular mechanical pattern in patients undergoing mitral valve surgery: a predictor of post-operative dysfunction?* ESC Heart Failure, 2020. **7**(3): p. 1246-1256.

42. Kovács, A., B. Lakatos, M. Tokodi, and B. Merkely, *Right ventricular mechanical pattern in health and disease: beyond longitudinal shortening.* Heart Failure Reviews, 2019. **24**(4): p. 511-520.

43. Stähli, B.E., C. Gebhard, P. Biaggi, S. Klaassen, E. Valsangiacomo Buechel, C.H. Attenhofer Jost, R. Jenni, F.C. Tanner, and M. Greutmann, *Left ventricular non-compaction: prevalence in congenital heart disease.* Int J Cardiol, 2013. **167**(6): p. 2477-81.
44. Kiss, A.R., Z. Gregor, A. Furak, A. Toth, M. Horvath, L. Szabo, C. Czimbalmos, Z. Dohy, B. Merkely, H. Vago, et al., *Left ventricular characteristics of noncompaction phenotype patients with good ejection fraction measured with cardiac magnetic resonance.* Anatol J Cardiol, 2021. **25**(8): p. 565-571.
45. Thuny, F., A. Jacquier, B. Jop, R. Giorgi, J.Y. Gaubert, J.M. Bartoli, G. Moulin, and G. Habib, *Assessment of left ventricular non-compaction in adults: side-by-side comparison of cardiac magnetic resonance imaging with echocardiography.* Arch Cardiovasc Dis, 2010. **103**(3): p. 150-9.
46. Hotta, V.T., M. Martinelli Filho, C. Mady, W. Mathias, and M.L.C. Vieira, *Comparison between 2D and 3D echocardiography in the evaluation of reverse remodeling after CRT.* Arquivos brasileiros de cardiologia, 2011. **97 2**: p. 111-21.
47. Gruszczynska, K., L.J. Krzych, K.S. Golba, J. Biernat, T. Roleder, M.A. Deja, P. Ulbrych, M. Malinowski, P. Janusiewicz, S. Wos, et al., *Statistical agreement of left ventricle measurements using cardiac magnetic resonance and 2D echocardiography in ischemic heart failure.* Med Sci Monit, 2012. **18**(3): p. MT19-25.
48. Bicudo, L.S., J.M. Tsutsui, A. Shiozaki, C.E. Rochitte, E. Arteaga, C. Mady, J.A. Ramires, and W. Mathias, Jr., *Value of real time three-dimensional echocardiography in patients with hypertrophic cardiomyopathy: comparison with two-dimensional echocardiography and magnetic resonance imaging.* Echocardiography, 2008. **25**(7): p. 717-26.
49. Pouleur, A.C., J.B. le Polain de Waroux, A. Pasquet, B.L. Gerber, O. Gerard, P. Allain, and J.L. Vanoverschelde, *Assessment of left ventricular mass and volumes by three-dimensional echocardiography in patients with or without wall motion abnormalities: comparison against cine magnetic resonance imaging.* Heart, 2008. **94**(8): p. 1050-7.
50. Pryds, K., A.H. Larsen, M.S. Hansen, A.Y.K. Grøndal, R.S. Tougaard, N.H. Hansson, T.S. Clemmensen, B.B. Løgstrup, H. Wiggers, W.Y. Kim, et al.,

Myocardial strain assessed by feature tracking cardiac magnetic resonance in patients with a variety of cardiovascular diseases – A comparison with echocardiography. Scientific Reports, 2019. **9**(1): p. 11296.

51. Erley, J., D. Genovese, N. Tapaskar, N. Alvi, N. Rashedi, S.A. Besser, K. Kawaji, N. Goyal, S. Kelle, R.M. Lang, et al., *Echocardiography and cardiovascular magnetic resonance based evaluation of myocardial strain and relationship with late gadolinium enhancement.* J Cardiovasc Magn Reson, 2019. **21**(1): p. 46.
52. Erley, J., R. Tanacli, D. Genovese, N. Tapaskar, N. Rashedi, P. Bucius, K. Kawaji, I. Karagodin, R.M. Lang, S. Kelle, et al., *Myocardial strain analysis of the right ventricle: comparison of different cardiovascular magnetic resonance and echocardiographic techniques.* Journal of Cardiovascular Magnetic Resonance, 2020. **22**(1): p. 51.
53. Bernard, A., K. Addetia, R. Dulgheru, L. Caballero, T. Sugimoto, N. Akhaladze, G.D. Athanassopoulos, D. Barone, M. Baroni, N. Cardim, et al., *3D echocardiographic reference ranges for normal left ventricular volumes and strain: results from the EACVI NORRE study.* Eur Heart J Cardiovasc Imaging, 2017. **18**(4): p. 475-483.
54. Szűcs, A., A.R. Kiss, Z. Gregor, M. Horváth, A. Tóth, Z. Dohy, L.E. Szabó, F.I. Suhai, B. Merkely, and H. Vágó, *Changes in strain parameters at different deterioration levels of left ventricular function: A cardiac magnetic resonance feature-tracking study of patients with left ventricular noncompaction.* Int J Cardiol, 2021. **331**: p. 124-130.
55. Kalapos, A., P. Domsik, T. Forster, and A. Nemes, *Comparative evaluation of left ventricular function by two-dimensional echocardiography and three-dimensional speckle-tracking echocardiography in noncompaction cardiomyopathy. Results from the MAGYAR-Path Study.* Orvosi Hetilap, 2013. **154**(34): p. 1352-1359.
56. Sanz, J., D. Sanchez-Quintana, E. Bossone, H.J. Bogaard, and R. Naeije, *Anatomy, Function, and Dysfunction of the Right Ventricle: JACC State-of-the-Art Review.* J Am Coll Cardiol, 2019. **73**(12): p. 1463-1482.
57. Vaidya, V.R., M. Lyle, W.R. Miranda, M. Farwati, A. Isath, S.H. Patlolla, D.O. Hodge, S.J. Asirvatham, S. Kapa, A.J. Deshmukh, et al., *Long-Term Survival of*

Patients With Left Ventricular Noncompaction. J Am Heart Assoc, 2021. **10**(2): p. e015563.

58. Zemrak, F., M.A. Ahlman, G. Captur, S.A. Mohiddin, N. Kawel-Boehm, M.R. Prince, J.C. Moon, W.G. Hundley, J.A. Lima, D.A. Bluemke, et al., *The relationship of left ventricular trabeculation to ventricular function and structure over a 9.5-year follow-up: the MESA study.* J Am Coll Cardiol, 2014. **64**(19): p. 1971-80.
59. Shehata, I.E., A.S. Eldamanhory, and A. Shaker, *Early predictors of left ventricular dysfunction in hypertensive patients: comparative cross-section study.* Int J Cardiovasc Imaging, 2020. **36**(6): p. 1031-1040.
60. Eslami, V., F. Bayat, B. Asadzadeh, E. Saffarian, A. Gheymati, E. Mahmoudi, and M.R. Movahed, *Early prediction of ventricular functional recovery after myocardial infarction by longitudinal strain study.* Am J Cardiovasc Dis, 2021. **11**(4): p. 471-477.
61. Stämpfli, S.F., A. Gotschy, P. Kiarostami, T. Özkartal, C. Gruner, M. Niemann, R. Manka, and F.C. Tanner, *Right ventricular involvement in left ventricular non-compaction cardiomyopathy.* Cardiol J, 2022. **29**(3): p. 454-462.
62. Antoni, M.L., R.W. Scherptong, J.Z. Atary, E. Boersma, E.R. Holman, E.E. van der Wall, M.J. Schalij, and J.J. Bax, *Prognostic value of right ventricular function in patients after acute myocardial infarction treated with primary percutaneous coronary intervention.* Circ Cardiovasc Imaging, 2010. **3**(3): p. 264-71.
63. Santamore, W.P. and L.J. Dell'Italia, *Ventricular interdependence: significant left ventricular contributions to right ventricular systolic function.* Prog Cardiovasc Dis, 1998. **40**(4): p. 289-308.
64. Wang, W., W. Chen, X. Lin, and L. Fang, *Influence of Right Ventricular Dysfunction on Outcomes of Left Ventricular Non-compaction Cardiomyopathy.* Front Cardiovasc Med, 2022. **9**: p. 816404.
65. Surkova, E., A. Kovács, M. Tokodi, B.K. Lakatos, B. Merkely, D. Muraru, A. Ruocco, G. Parati, and L.P. Badano, *Contraction Patterns of the Right Ventricle Associated with Different Degrees of Left Ventricular Systolic Dysfunction.* Circulation: Cardiovascular Imaging, 2021. **14**(10): p. e012774.

66. Gregor, Z., A. Kiss, K. Grebur, Z. Dohy, A. Kovács, B. Ph.D, H. Vago, and A. Szűcs, *Characteristics of the right ventricle in left ventricular noncompaction with reduced ejection fraction in the light of dilated cardiomyopathy*. PLOS ONE, 2023. **18**: p. e0290981.

9. Bibliography of the candidate's publications

9.1. Publications related to the dissertation

1. Horváth M, Kiss D, Márkusz I, Tokodi M, Kiss AR, Gregor Z, et al. Comparison of imaging modalities for left ventricular noncompaction morphology. J Imaging. 2025;11(6):185.
   IF (2025): 3.3
2. Horváth M, Farkas-Süto K, Fábián A, Lakatos B, Kiss AR, Grebur K, et al. Highlights of right ventricular characteristics of left ventricular noncompaction using 3D echocardiography. IJC Heart Vasc. 2023;41:101289.
   IF (2023): 2.28
3. Horváth M, Farkas-Süto K, Gyulánczi FK, Fabián A, Lakatos B, Kiss AR, et al. 3D echocardiographic assessment of right ventricular involvement of left ventricular hypertrabecularization from a new perspective. J Imaging. 2025;11(6):181.
   IF (2025): 3.3

9.2. Publications not related to the dissertation

1. Grebur K, Mester B, Fekete BA, Kiss AR, Gregor Z, Horváth M, et al. Genetic, clinical and imaging implications of a noncompaction phenotype population with preserved ejection fraction. Front Cardiovasc Med. 2024;11:1337378.
   IF (2024): 2.9
2. Szucs A, Kiss AR, Gregor Z, Horváth M, Tóth A, Dohy Z, et al. Changes in strain parameters at different deterioration levels of left ventricular function: A cardiac magnetic resonance feature-tracking study of patients with left ventricular noncompaction. Int J Cardiol. 2021;328:1-9.
   IF (2021): 2.46
3. Kiss AR, Gregor Z, Furak A, Tóth A, Horváth M, Szabó L, et al. Left ventricular characteristics of noncompaction phenotype patients with good ejection fraction measured with cardiac magnetic resonance. Anatol J Cardiol. 2021;25(3):196-203.

IF (2021): 1.5

4. Babity M, Zamodics M, Konig A, Kiss AR, Horvath M, Gregor Z, et al. Cardiopulmonary examinations of athletes returning to high-intensity sport activity following SARS-CoV-2 infection. Sci Rep. 2022;12:24486.
   IF (2022): 4.44
5. Grebur K, Gregor Z, Kiss AR, Horváth M, Mester B, Czimbalmos C, et al. Different methods, different results? Threshold-based versus conventional contouring techniques in clinical practice. Int J Cardiol. 2023;371:123-31.
   IF (2023): 2.20
6. Grebur K, Mester B, Horváth M, Farkas-Sütö K, Gregor Z, Kiss AR, et al. The effect of excessive trabeculation on cardiac rotation: A multimodal imaging study. PLoS One. 2024;19(4):e0308035.
   IF (2024): 2.6
7. Gregor Z, Kiss AR, Szabó LE, Tóth A, Grebur K, Horváth M, et al. Sex- and age-specific normal values of left ventricular functional and myocardial mass parameters using threshold-based trabeculae quantification. PLoS One. 2021;16(10):e0258362.
   IF (2021): 3.75
8. Zamodics M, Babity M, Schay G, Bucsko-Varga A, Kovacs E, Horvath M, et al. Investigation of body composition and cardiac sports adaptation in elite water polo players. Sports (Basel). 2025;13(6):180.
   IF (2025): 2.9
9. Komlósi F, Arnóth B, Szakál I, Tóth P, Mészáros H, Sánta H, et al. Comparative analysis of therapeutic strategies in atrial fibrillation patients with left atrial appendage thrombus despite optimal NOAC therapy. Clin Res Cardiol. 2025;Epub ahead of print.
   IF (2025): 3.7

10. Acknowledgments

I would like to express my deep gratitude to Professor Dr. Béla Merkely for his outstanding professional example and leadership. It has been a privilege to conduct my research in such a high-level academic and clinical environment, where scientific excellence and patient-centered care are equally prioritized.

I am profoundly grateful to my supervisor, Dr. Andrea Szűcs, for her endless patience, unwavering support, and invaluable guidance throughout my doctoral work. Her mentorship extended far beyond the research process, shaping my development both within the echocardiography working group and in everyday clinical practice. Her critical insight, encouragement, and trust were fundamental to the completion of this thesis.

I would also like to sincerely thank the members of our working group, Dr. Anna Réka Kiss, Dr. Zsófia Gregor, Dr. Kristóf Farkas-Sütő, Dr. Balázs Mester, and Dr. Flóra Gyulánczi, for the countless hours of collaborative work, shared scientific discussions, and memorable moments of friendship. The professional synergy and supportive atmosphere we created together made this journey not only productive but genuinely enjoyable.

Finally, I owe my deepest appreciation to my family and to my partner for their unconditional support, patience, and encouragement. Their belief in me provided the stability and motivation necessary to complete this work.